THE UNIVERSITY OF MICHIGAN

INDUSTRY PROGRAM OF THE COLLEGE OF ENGINEERING

AN ASYMPTOTIC SOLUTION TO A PROBLEM IN SHELL STABILITY

Robert L. Armstrong

A dissertation submitted in partial fulfillment
of the requirements for the degree of
Doctor of Philosophy in the
University of Michigan
Department of Engineering Mechanics
1964

October, 1964

IP-682

Doctoral Committee:

Professor Ernest F. Masur, Chairman
Professor Robert M. Haythornthwaite
Professor Albert E. Heins
Assistant Professor Ivor K. McIvor

ACKNOWLEDGMENTS

The author wishes to express his sincere appreciation to his Chairman, Professor Ernest F. Masur for his patient encouragement and his excellent instruction, and also to the other members of his committee for their interest and time.

The author also wishes to thank the National Aeronautics and Space Administration for their financial support and the Industry Program of the College of Engineering for their assistance in the reproduction of this work.

TABLE OF CONTENTS

LIST OF FIGURES

NOMENCLATURE

A_1	parameter $\left(A_1 = \sqrt{1+\frac{P/P_E}{(1-2k)}}\right)$
A_2	parameter $\left(A_2 = \sqrt{1-\frac{P/P_E}{(1-2k)}}\right)$
A_3	parameter $\left(A_3 = \sqrt{1+\sqrt{1-\left(\frac{1-2k}{P/P_E}\right)^2}}\sqrt{\frac{2P/P_E}{(1-2k)}}\right)$
A_4	parameter $\left(A_4 = \sqrt{1-\sqrt{1-\left(\frac{1-2k}{P/P_E}\right)^2}}\sqrt{\frac{2P/P_E}{(1-2k)}}\right)$
D	flexural rigidity of the shell
E	Young's modulus
F	stress function referred to Π_1
F'	stress function referred to Π_2
$N_{\alpha\beta}$	additional stress resultants referred to Π_1
$N'_{\alpha\beta}$	additional stress resultants referred to Π_2
$N^\circ_{\alpha\beta}$	prebuckling stress resultants
$N'_{\rho\rho}$, $N'_{\zeta\rho}$, $N'_{\zeta\zeta}$	additional stress resultants referred to Π_2
P	applied axial stress resultant
$\overline{P}$	nondimensional P $\left(\overline{P} = \frac{PR}{Eh^2}\right)$
P_E	classical buckling load
R	radius of prebuckled cylinder
dS	element of surface area
S_T	surface area where tractions are specified
$\hat{T}$	surface traction vector
T_R	force along a ridge

T_{Rz}, T_{Rx}	z and x components of T_R
T_v	force along a valley
T_{vz}	z component of T
V	potential energy change during buckling
V_w	potential energy change of existing stresses during buckling
V_m	potential energy change due to membrane stresses
V_B	potential energy change due to bending stresses
W	deflection of the prebuckled shell from Π_1
W'	deflection of the prebuckled shell from Π_2
Y	nondimensional W $\quad (Y = \frac{W}{nh})$
Y'	nondimensional W' $\quad (Y' = \frac{W'}{nh})$
a_1	parameter $\quad (a_1 \approx \frac{\pi^2 R}{6n^2}(1 - k^2))$
a_2	parameter $\quad (a_2 \approx \frac{\pi^2 R}{6n^2}(1 - k^2))$
a_3	parameter $\quad (a_3 \approx \frac{\pi^2 R}{6n^2}(2 + k^2))$
a_4	parameter $\quad (a_4 \approx \frac{\pi^2 R}{2n^2} k)$
a_5	parameter $\quad (a_5 \approx \frac{\pi^2 R}{8n^2})$
b_i $\quad (i = 1, 2, \ldots. 8)$	constants of integration
c_i $\quad (i = 1, 2, \ldots. 8)$	constants of integration
d_i $\quad (i = 1, 2, \ldots. 8)$	constants of integration
f	nondimensional F $\quad (f = \frac{F}{nEh^2})$

f'	nondimensional F' $\left(f' = \frac{F'}{nEh^2}\right)$
g	parameter $\left(g = \frac{n^3 h}{R}\right)$
h	shell thickness
k	deformation parameter
$\bar{k}$	parameter $\left(\bar{k} = \frac{8\mu^2\alpha_4}{(1+\mu^2)^2}\right.$
l	representative buckled shell dimension
ℓ_x, ℓ_s	axial and circumferential buckled shell wave lengths
m	parameter indicating the magnitude of the stress in the field
$\bar{m}$	parameter $\left(\bar{m} = \frac{\mu^2 \ell_s^2 m}{(1+\mu^2)^2 \ell^2}\right.$)
n	number of circumferential buckles
p	parameter $\left(p^2 = 1 - \frac{4\gamma^2 k^2}{m^2 \bar{p}^2}\right)$
q	parameter $\left(q^2 = \frac{4\gamma^2 k^2}{m^2 \bar{p}^2} - 1\right)$
s	circumferential coordinate in Π_1
$\bar{s}$	circumferential coordinate in Π_2
$\hat{s}$	nondimensional s $\left(\hat{s} = \frac{2s}{\ell_s}\right)$
t	parameter $\left(t = \frac{\pi\mu}{2g\gamma}\sqrt{kn}\right)$
u_α	components of the displacement of shell middle surface
$\hat{u}_\alpha$	components of the displacement of a general point
$\hat{u}$	displacement vector
dv	volume element of the shell
w	displacement of the shell middle surface normal to Π_1
w'	displacement of the shell middle surface normal to Π_2

$\hat{w}$	displacement of a general point
w_r	radial displacement of the shell middle surface
x	axial coordinate in Π_1
$\bar{x}$	axial coordinate in Π_2
$\hat{x}$	nondimensional $(x = \frac{2x}{\ell_x})$
y	nondimensional w $(y = \frac{w}{nh})$
y'	nondimensional w' $(y' = \frac{w'}{nh})$
y_i, y_i' $(i = 0, 1, 2, \ldots)$	components of y_i and y_i'
y_{ij} $(i = 1,2,\ldots, j = 1,2,..)$	components of y_i and y_i'
z	coordinate normal to Π_1
z'	coordinate normal to Π_2
$\overset{)}{\nabla}{}^4$, $\overset{-}{\nabla}{}^4$, $\overset{=}{\nabla}{}^4$	differential operators
Π_1, Π_2	reference planes
χ	angle
α_i $(i = 1, 2, \ldots 5)$	nondimensional a_i $(\alpha_i = \frac{a_i}{nh})$
γ	parameter $(\gamma^2 = \frac{1}{12(1 - \nu^2)})$
$\delta_{\alpha\beta}$	Kronecker delta
δ	parameter $(\delta^2 = \frac{1}{n})$
$\epsilon_{\alpha\beta}$	additional strain components
ζ	nondimensional coordinate $(\zeta = \frac{\bar{x}}{\ell_x} - \frac{\bar{s}}{\ell_s} + \frac{1}{2}$
η	nondimensional coordinate $(\eta = \frac{\zeta}{\delta})$
θ	parameter
λ	parameter $(\lambda = \sqrt{2k}/\gamma$
$\bar{\lambda}$	parameter $(\bar{\lambda} = \sqrt{2\bar{k}}/\gamma$
$\hat{\lambda}_i$ $(i = 1, 2, \ldots 8)$	parameter

μ	aspect ratio of a buckle $\left(\mu = \frac{\ell_x}{\ell_s}\right)$
ν	Poisson's ratio
ξ	nondimensional coordinate $\left(\xi = \frac{x}{\ell}\right)$
ρ	nondimensional coordinate $\left(\rho = \frac{\bar{x}}{\ell_x} + \frac{\bar{s}}{\ell_s} + \frac{1}{2}\right)$
σ	nondimensional coordinate $\left(\sigma = \frac{s}{\ell}\right)$
$\tau_{\alpha\beta}$	additional stress components at a general point
$\tau^{\circ}_{\alpha\beta}$	prebuckling stress components at a general point
ψ	nondimensional coordinate $\left(\psi = \frac{\xi}{\delta}\right)$

Subscripts α, β, and γ take on the values x and s. If any of these subscripts are repeated the quantity is summed.

CHAPTER I

INTRODUCTION

The problems of determining theoretically the conditions under which a thin circular shell under axial compression becomes unstable, and of determining the postbuckling behavior of the shell have been of interest to engineers and scientists for nearly sixty years.

The first theoretical work on this problem was done by such noted investigators as Lorentz[1], Timoshenko[2], Southwell[3], and Flügge[4]. They found what might be called the classical or Euler buckling load. This is the load at which an equilibrium configuration differing from the initial configuration by an infinitesimal displacement can be found. In other words, it is the load at which a bifurcation in the load-axial deflection curve exists.

When a cylindrical shell buckles, the change in the potential energy of the shell can be expressed as a sum of second, third, and fourth order terms in the radial displacement, w_r . The equilibrium equation in the radial direction can be found by setting the first variation of this additional potential energy equal to zero. If only the second order terms are used, the resulting equilibrium equation is linear. The resulting system is homogeneous, and the lowest value of axial load for which a nontrivial solution exists is the Euler load, P_E . In terms of force per unit length of shell circumference this is given by

$$P_E = 2\gamma \frac{Eh^2}{R} = .605 \frac{Eh^2}{R} \quad (\nu = .30). \tag{1.1}$$

(For a solution of the linear problem, see Timoshenko and Gere[5].)

Experimental work, however, indicates that cylindrical shells under axial compression fail at values of axial stress only one tenth to nine tenths the Euler load. Along with this sharp reduction in the actual strength of the shell a wide range of scatter is also observed. This is indicated in Figure 1.1. (Donnell and Wan[14].)

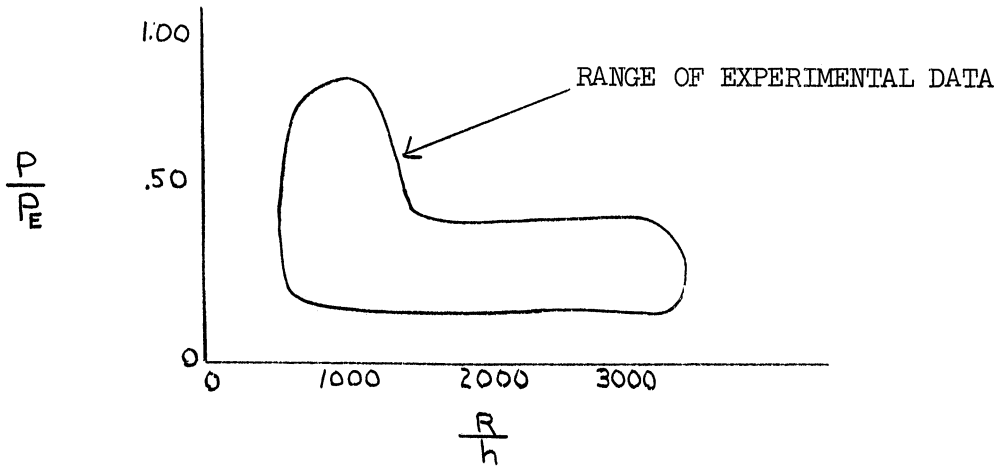

Figure 1.1. Range of Experimental Values for the Buckling Load.

Thin cylinders under axial load buckle either generally into a pattern consisting of a large number of circumferential and axial rows of diamond-shaped buckles, or they buckle locally into isolated buckles or into only a few axial rows of circumferential buckles. As buckling progresses the number of circumferential buckles (n) decreases, the value of n being near ten for cylinders which buckle in the manner described. The final buckled shape is observed to consist of regions of small curvature connected by ridges and valleys of very high curvature. This is easily seen in the photographs shown by Fung and Sechler[6] and by

Lundquist[7]. This is the postbuckled shape which is analyzed in this work.

An explanation of the discrepancy between theory and experiment has been attempted by several investigators. Donnell[8], in 1934, was the first to use a finite-deflection analysis which included the effect of initial imperfections. Unfortunately his work was not general enough and attracted therefore only limited attention. Von Kármán and Tsien[9], in 1941, extending the idea of Donnell, also considered finite displacements from the prebuckled cylinder. They found equilibrium states which could exist at values of axial stress much less than the buckling load. This method was refined and extended among others by Leggett and Jones[10], Michielson[11], Kempner[12], and finally by Almroth[13] in 1963. Almroth showed that a possible equilibrium state can exist when the external load is only ten per cent of the Euler load.

An answer to the question of how the shell reaches its postbuckled state, which seems to account for the wide scatter in experimental data, was put forth by Donnell and Wan[14] in 1950. They postulated an initially imperfect shell, the initial imperfections being of the same form as the buckled shape. They determined that the shell was very sensitive to these imperfections. A series of load-deformation curves were found for various values of the imperfection parameter. (See Figure 1.2.)

Koiter[15] demonstrated the extreme sensitivity of cylindrical shells to imperfections by showing that the curve giving the buckling load as a function of the imperfections amplitude may have infinite slope as the latter approaches zero.

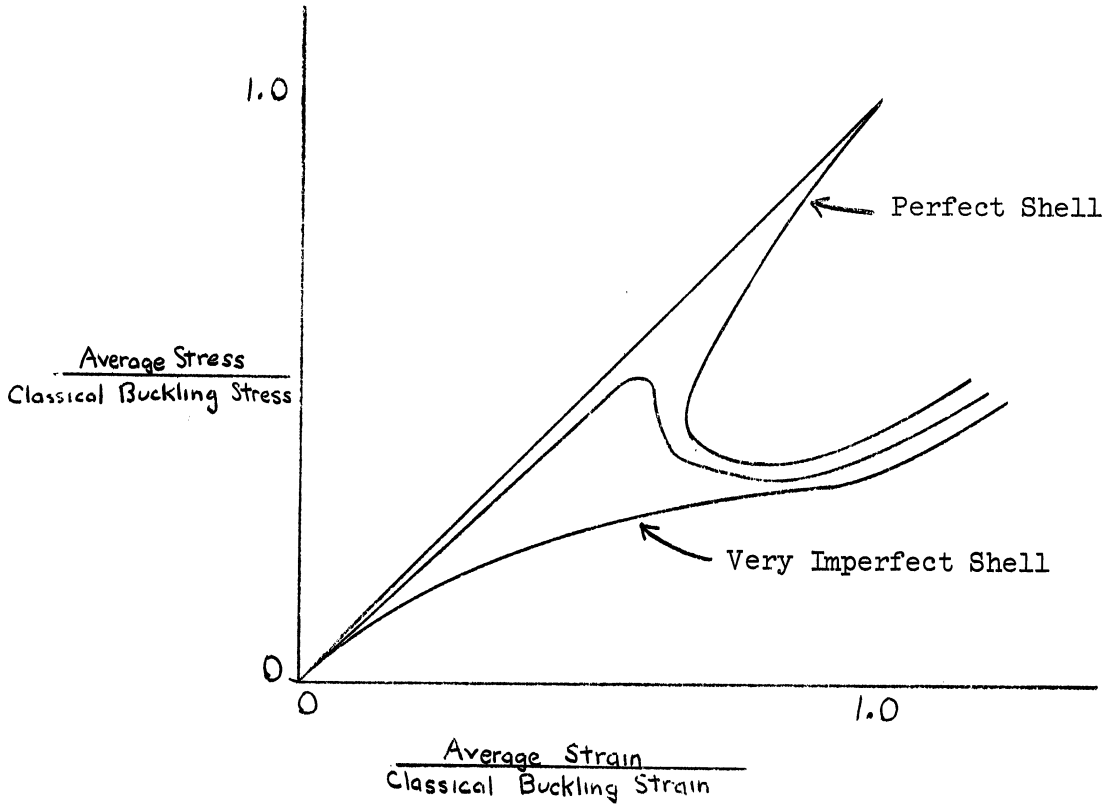

Figure 1.2. Effect of Shell Imperfections on the Buckling Behavior.

Several investigators have investigated the dynamics of the postbuckling problem, such as Kadashevich and Pertsov[16], Agamirov and Volmir[17], and Yao[18]. The results of these studies have shed no significant light on the basic controversy and are therefore not discussed here any further.

It is of significance in connection with the present work that none of the previous investigations cited here represent exact solutions to the relevant shell equations, whose nonlinearity has made an exact analysis prohibitively difficult. Instead, the approach which has been

utilized most widely to obtain approximate solutions has been to set up an expression for the potential energy and to minimize that expression within an aggregate of kinematically admissible deflection functions. This is, of course, a permissible scheme, provided that the number of function considered is sufficiently large and the functions themselves represent good approximations. In particular, if the actual deflected surface is sufficiently smooth, an aggregate of trigonometric functions is usually workable. If sharp discontinuities in the functions or their derivatives occur convergence becomes slow or altogether questionable.

This phenomenon has been observed in the present case, in which the addition of ever increasing numbers of terms has led to approximate solutions of formidable algebraic complexity without displaying satisfactory convergence as the deflections become large. It may be conjectured that this is a basic shortcoming of the method selected. Indeed, the observed presence of diamond-shaped buckles separated by sharp creases (or internal "boundary layers", as discussed later on) raises the question of the suitability of the representation by an aggregate of simple trigonometric waves.

The method employed herein is also approximate, but in a different sense. Energy techniques are not employed. Instead, the shell equations are solved approximately through perturbation expansion in terms of a small parameter which is related to the thickness of the shell. Since this parameter (after a number of order-of-magnitude assumptions based on observed behavior) appears as the coefficient of the highest

derivatives in the equations, the expansion is singular and gives rise to boundary layers separating "fields" of relatively smooth buckles of vanishing Gaussian curvature. Aside from certain inaccuracies in satisfying some of the kinematic boundary conditions (believed to be of minor significance), the solutions obtained, though not unique, may therefore be considered exact in the limit, that is, as the shell thickness approaches zero.

The idea of using a boundary layer approach to problems in shell stability is not new. Friedrichs[19], in 1941, investigated the problem of the buckling of a spherical cap by using a boundary layer analysis. Other early work using boundary layer analyses in the investigation of the behavior of structures was done by Friedrichs and Stoker[20,21] in connection with the problem of a circular plate under uniform radial compression. More recently the development of a boundary layer in a flat plate with free edges has been investigated by Fung and Wittrick[22] and by Masur and Chang.[23] There are also examples of boundary layer analyses in the investigation of problems of linear shell theory. See, for example, the recent work of Reiss,[24,25] and Johnson[26] in the treatment of the linear problem of a cylindrical shell under axial compression.

The development of internal boundary layers in cylindrical shell buckling is suggested by the observed buckled shape. The boundary layers are those regions which include the valleys and ridges which delineate the individual buckles. It is expected that there will be large bending strains in the boundary layers, but that the bending will be almost negligible in the "field" (the region remote from the boundary layers). This behavior has been noted by several investigators. (For example, see Fung and Sechler[6]).

The present investigation is in the spirit of von Kármán and Tsien in that equilibrium states for the postbuckled shell are sought. An initially perfect cylinder is postulated, although the results can also be shown to be valid for an imperfect cylinder. Another feature of this work is that by considering each buckle as a shallow shell both the local and general buckling problem are investigated simultaneously.

CHAPTER II

DERIVATION OF THE SHELL EQUATIONS

Consider a shell of constant thickness, h, whose initial middle surface is defined by the relationship

$$W = W(x,s). \tag{2.1}$$

The coordinates x and s are chosen to lie in a reference plane Π_1; the distance of the middle surface from Π_1 being W. W is measured in the z direction which is normal to Π_1 (Figure 2.1).

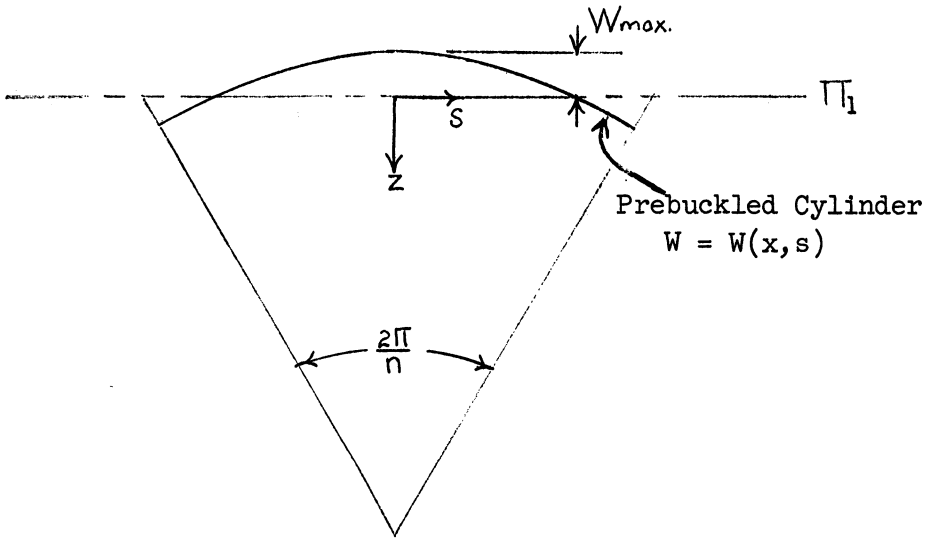

Figure 2.1. Axial Section Showing the Prebuckled Panel.

It is assumed that for the shell considered

$$\frac{W_{max}}{l} \ll 1 \tag{2.2}$$

in which ℓ is a representative shell dimension and W_{max} is the maximum rise of the shell from Π_1. This type of shell is commonly called a shallow shell. Another way of considering the shell is to think of it as a plate with an initial deflection.

The Love-Kirchoff assumptions concerning the deformations of the shell are made. The shear deformation is therefore neglected. Also, the volume element of the shell is taken to be

$$dV = dx\, ds\, dz \tag{2.3}$$

which is consistant with Love's first approximation and the usual shallow shell theory.

It follows from the Love-Kirchoff assumptions and the assumption (2.2) that the displacement components of a general point in terms of the middle surface displacement components are

$$\left.\begin{aligned} \hat{U}_\alpha(x,s,z) &= U_\alpha - z W_{,\alpha} \\ \hat{W}(x,s,z) &= W \end{aligned}\right\} \qquad \alpha = x,s \tag{2.4}$$

in which the tangential displacements u_α and the normal displacements w of the middle surface are functions of x and s only. (The summation convention is adopted for the subscripts α, β and γ; the range of subscripts is indicated in (2.4).)

For the deformations being considered the displacement components u_α are taken to be of an order-of-magnitude smaller than the displacement component w, that is,

$$\left.\begin{aligned} w &\sim O(nh)^* \\ u_\alpha &\sim O(h) \end{aligned}\right\} \tag{2.5}$$

in which n is an integer such that

$$W_{max} \sim O(nh). \tag{2.6}$$

As a consequence of the order-of-magnitude assumptions which have been made a shallow shell theory with deflections of the order-of-magnitude of the shell rise is being considered. For a circular cylindrical shell the shallow shell being considered is one of the diamond-shaped buckled panels. For such a shell n is taken to be the number of circumferential buckles.

The strains are expressed in terms of the middle surface displacements as follows,

$$\hat{\epsilon}_{\alpha\beta} = \frac{1}{2}\left[u_{\alpha,\beta} + u_{\beta,\alpha} + (w+W)_{,\alpha}(w+W)_{,\beta} - W_{,\alpha}W_{,\beta} - 2z\,w_{,\alpha\beta}\right]. \tag{2.7}$$

In the usual theory in which $w \sim O(h)$ the terms $w_{,\alpha}\, w_{,\beta}$ and $zw_{,\alpha\beta}$ are both $O\left(\frac{h^2}{\ell^2}\right)$. For the displacements considered here, however, $zw_{,\alpha\beta}$ is $O\left(n\frac{h^2}{\ell^2}\right)$ while $w_{,\alpha}\, w_{,\beta}$ is $O\left(n^2\frac{h^2}{\ell^2}\right)$; thus the term $zw_{,\alpha\beta}$ is

* The expression $w \sim O(nh)$ should be interpreted to mean that maximum values of the displacement approximately n times the shell thickness are expected.

of an order-of-magnitude smaller than the other terms. However, because of the higher derivatives involved this term becomes significant in a boundary layer whereas other terms which have been neglected in (2.7) and which are of similar order to the bending term involve lower order derivatives and remain small when compared to the membrane terms, even in the boundary layers.

For a given load the difference in the potential energy between the buckled and unbuckled state is given by the expression

$$V = \int_V \left[\hat{\tau}^{\circ}_{\alpha\beta} \hat{\epsilon}_{\alpha\beta} + \frac{1}{2} \hat{\tau}_{\alpha\beta} \hat{\epsilon}_{\alpha\beta} \right] dV - \int_{S_T} \hat{T} \cdot \hat{U} \, dS \tag{2.8}$$

in which $\tau_{\alpha\beta}$ are the additional stress components which arise during buckling and $\tau^{o}_{\alpha\beta}$ are the prebuckling stress components. $\hat{T}$ is a vector which represents the applied surface tractions and $\hat{U}$ is a vector which represents the displacements through which the tractions act.

The work done by the external tractions is equal to the work of the prebuckling stresses acting through the linear portion of the additional strains. The potential energy change can therefore be written

$$V = V_w + V_B + V_m \tag{2.9}$$

in which

$$V_w = \frac{1}{2} \int N^{\circ}_{\alpha\beta} w_{,\alpha} w_{,\beta} \, dS. \tag{2.10}$$

$$V_B = \frac{D}{2}\int\left[(1-\nu)\, w_{,\alpha\beta} w_{,\alpha\beta} + \nu\, w_{,\alpha\alpha}\, w_{,\beta\beta}\right] dS \tag{2.11}$$

$$V_m = \frac{1}{2}\int N_{\alpha\beta}\,\epsilon_{\alpha\beta}\; dS. \tag{2.12}$$

$N^{o}_{\alpha\beta}$ and $N_{\alpha\beta}$ are defined by

$$N^{o}_{\alpha\beta} \equiv \int_{-\frac{h}{2}}^{\frac{h}{2}} \hat{\tau}^{o}_{\alpha\beta}\; dz$$

$$N_{\alpha\beta} \equiv \int_{-\frac{h}{2}}^{\frac{h}{2}} \hat{\tau}_{\alpha\beta}\; dz \tag{2.13}$$

In obtaining (2.11) it has been assumed that the additional strains are related to the additional stresses by Hooke's law for plane stress, that is,

$$\hat{\tau}_{\alpha\beta} = \frac{E}{(1-\nu^2)}\left[(1-\nu)\hat{\epsilon}_{\alpha\beta} + \nu\,\hat{\epsilon}_{\gamma\gamma}\,\delta_{\alpha\beta}\right]. \tag{2.14}$$

The additional stress resultants in terms of the middle surface displacements for a material with a stress strain law as given in (2.14) are

$$N_{\alpha\beta} = \frac{Eh}{(1-\nu^2)}\left[\frac{(1-\nu)}{2}\left(u_{\alpha,\beta}+u_{\beta,\alpha}+(w+W)_{,\alpha}(w+W)_{,\beta}-W_{,\alpha}W_{,\beta}\right.\right.$$

$$\left.\left.+\frac{\nu}{2}\left(2u_{\gamma,\gamma}+(w+W)_{,\gamma}(w+W)_{,\gamma}-W_{,\gamma}W_{,\gamma}\right)\delta_{\alpha\beta}\right]. \qquad (2.15)$$

The additional middle surface strains are

$$\epsilon_{\alpha\beta} = \frac{1}{2}\left[u_{\alpha,\beta}+u_{\beta,\alpha}+(w+W)_{,\alpha}(w+W)_{,\beta}-W_{,\alpha}W_{,\beta}\right]. \qquad (2.16)$$

The equilibrium equations are obtained by equating the first variation of the additional potential energy to zero, that is,

$$\left.\begin{aligned}\delta_{u_\alpha} V &= 0\\ \delta_w V &= 0.\end{aligned}\right\} \qquad (2.17)$$

These lead to

$$N_{\alpha\beta,\alpha} = 0 \qquad (2.18)$$

$$Dw_{,\alpha\alpha\beta\beta} - N^{\circ}_{\alpha\beta}w_{,\alpha\beta} - N_{\alpha\beta}(w+W)_{,\alpha\beta} = 0. \qquad (2.19)$$

Since $N_{\alpha\beta}$, rather than u_α, have been selected as dependent variables an additional equation (compatibility) must be added for

completeness. This equation is

$$N_{\alpha\alpha,\beta\beta} - N_{\alpha\beta,\alpha\beta} = \frac{Eh}{2}\left[(w+W)_{,\alpha\beta}(w+W)_{,\alpha\beta} - (w+W)_{,\alpha\alpha}(w+W)_{,\beta\beta} - W_{,\alpha\beta}W_{,\alpha\beta} + W_{,\alpha\alpha}W_{,\beta\beta}\right]. \tag{2.20}$$

The governing set of equations for the shallow shell thus consists of (2.18), (2.19), and (2.20).

Consider now a segment of a circular cylindrical shell. The original shell middle surface segment can be approximated by a parabola for segments which can be considered as shallow shells. The initial shape is given by the relation

$$W(x,s) = -a_3 + \frac{1}{2}\frac{s^2}{2R} \tag{2.21}$$

The prebuckling state of stress is taken to be one of uniform axial compression:

$$N^{\circ}_{xx} = -P \qquad N^{\circ}_{xs} = 0 \qquad N^{\circ}_{ss} = 0 \tag{2.22}$$

Equations (2.18) are satisfied identically if a stress function F is introduced by means of

$$N_{xx} = F_{,ss} \qquad N_{xs} = -F_{,xs} \qquad N_{ss} = F_{,xx} \tag{2.23}$$

In view of (2.21), (2.22), and (2.23), the shell equations are

$$\left.\begin{aligned} &D\nabla^4 w + P w_{,xx} - F_{,ss} w_{,xx} + 2F_{,xs} w_{,xs} - F_{,xx}\left(w_{,ss} + \frac{1}{R}\right) = 0 \\ &\nabla^4 F - Eh\left(w_{,xs}^2 - w_{,xx} w_{,ss} - \frac{1}{R} w_{,xx}\right) = 0. \end{aligned}\right\} \qquad (2.24)$$

Equations (2.24) are the Donnell equations for a cylindrical shell[8,27]. These equations are also Marguerre shallow shell equations for the special case of a cylindrical panel[28].

Equations (2.24) are usually consistant only for deflections of the order of the thickness of the shell. However, for modes of deformation which involve boundary layers these equations can be used for larger deflections.

CHAPTER III

SOLUTION OF THE SHELL EQUATIONS

3.1. Non-dimensional Form of the Shell Equations

The experimentally observed buckled shape for a thin cylindrical shell loaded in axial compression consists of a series of triangular shaped regions of nearly zero curvature separated by ridges and valleys of large curvature. These triangular regions form a set of n circumferential buckles. These buckles can extend over the entire lateral surface of the shell, or there may be only a few axial rows of buckles [6,7]. In the following analysis a typical buckle will be considered.

A drawing of an idealized buckle is shown in Figure 3.1. The reference plane, Π_1, is chosen so that the point (1) and (2) lie in Π_1 when the shell has buckled. The lines (01), (02), (13), and (23) represent ridges, while the line (12) represents a valley. The triangular fields (012) and (123) are assumed to retain some curvature in the buckled state. The unbuckled shell is shown by means of the dashed curve, the buckled shell by means of the solid curves. The parameter k is the ratio of the curvature of a buckled panel to the curvature of the original cylinder. $k = 0$ means that the "fields" are flat. $k = 1$ means there has been no deformation. a_1, a_2, a_3, and a_4 are parameters which aide in the description of the buckled panel. They are functions of R, k, and n.

The assumed buckled shape for the shell is almost developable. This fact can be rationalized if it is assumed that the buckled shape will be such as to minimize the potential energy of the shell. The

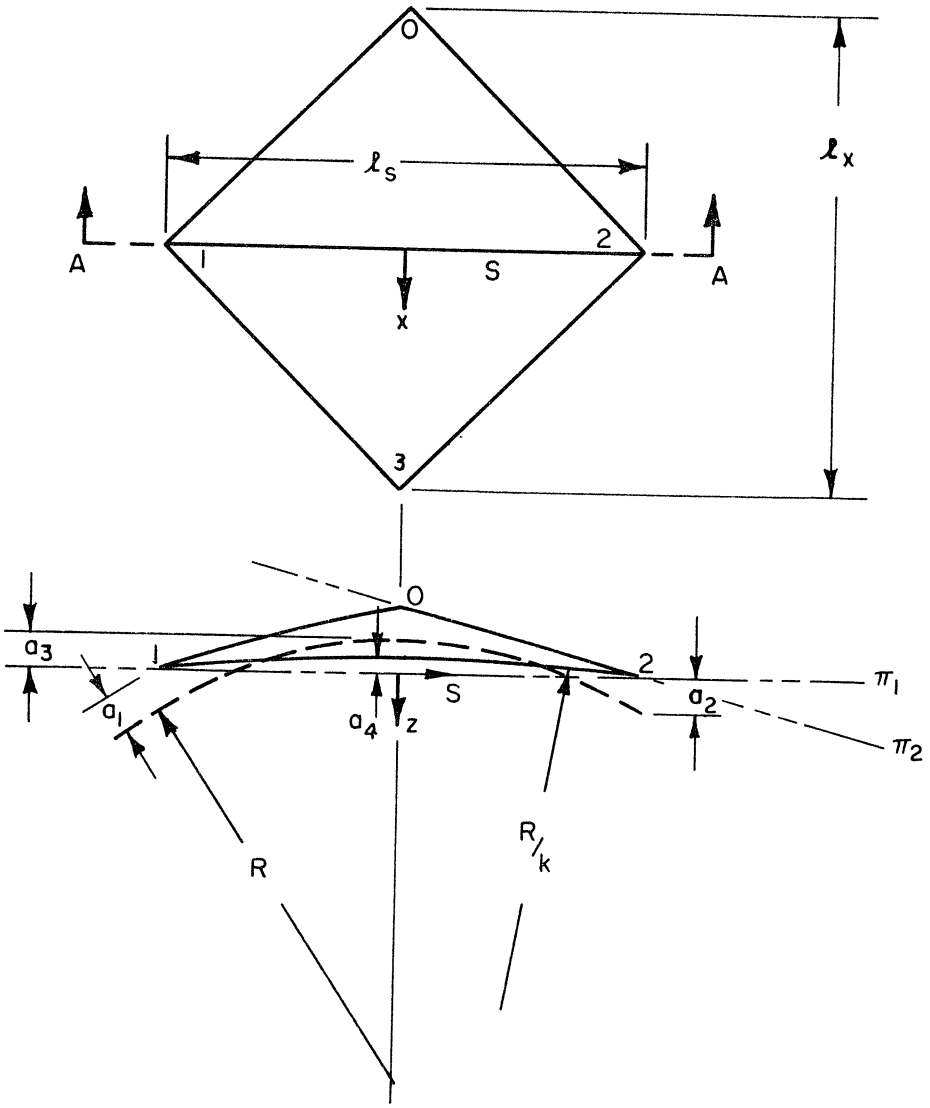

Section AA

Figure 3.1. Geometry of a Buckled Panel.

energy associated with membrane strains is proportional to the shell thickness, while the energy of bending is proportional to the cube of the shell thickness. Thus, since shells are of small thickness, the buckled shape will be one which minimizes the membrane strain energy, i.e., a developable surface. The developability of the buckled surface has been noted and discussed by several investigators.[29,30]

The assumption of developability allows the deformation parameters a_2, a_3, and a_4 to be expressed in terms of k, n, and the undeformed shell parameters R and h by using geometrical considerations alone (Appendix A). The results of doing this under the assumption that the angle is small are

$$\left.\begin{aligned} a_1 \approx a_2 &\approx (1-k^2)\frac{\pi^2 R}{6n^2} \\ a_3 &\approx (2+k^2)\frac{\pi^2 R}{6n^2} \\ a_4 &\approx k\frac{\pi^2 R}{2n^2}. \end{aligned}\right\} \qquad (3.1.1)$$

The membrane stresses in the regions remote from the boundaries are assumed to be uniform axial tension in the buckled state. A tensile stress is necessary for equilibrium. (See Appendix B).

Equation (2.24) can be put in nondimensional form in the following way. Because of the order of magnitude assumption concerning $w(x,s)$ and $W(x,s)$, let

$$\left.\begin{aligned} W &\equiv nhY \\ w &\equiv nhy. \end{aligned}\right\} \qquad (3.1.2)$$

The initial stress P is taken to be similar in magnitude to the buckling load as obtained from a linear analysis, that is,

$$P \sim O\left(\frac{Eh^2}{R}\right). \tag{3.1.3}$$

The radius of the undeformed shell is not, in general, representative of the deformed shape; rather, a more realistic choice of a representative of the deformed shape; rather, a more realistic choice of a representative length is made by means of

$$l^2 \equiv nRh. \tag{3.1.4}$$

In terms of l rather than R (3.1.3) becomes

$$P \sim O\left(\frac{nEh^3}{l^2}\right). \tag{3.1.5}$$

Dimensionless space variables are introduced by means of

$$\begin{aligned} x &\equiv \xi l \\ s &\equiv \sigma l. \end{aligned} \tag{3.1.6}$$

With the assumption that differentiation with respect to ξ and σ does not significantly change the magnitude of the function being differentiated and also on the basis of (3.1.5), let

$$P \equiv \frac{nEh^3}{l^2}\bar{P}. \tag{3.1.7}$$

Finally, define a nondimensional stress function f by means of

$$F \equiv nEh^3 f. \tag{3.1.8}$$

This choice implies that the additional stresses are of the same order as the original stresses.

Let

$$\left.\begin{aligned} a_2 &\equiv nh\alpha_2 & \nu &\equiv \frac{l_x}{l_s} \\ a_3 &\equiv nh\alpha_3 & \delta^2 &\equiv \frac{1}{n} \\ a_4 &\equiv nh\alpha_4 & \gamma^2 &= \frac{1}{12(1-\nu^2)} \\ l_s &\equiv \frac{2\pi R}{n} & \nabla^4 &\equiv \left[\frac{\partial^4}{\partial\xi^4} + 2\frac{\partial^4}{\partial\xi^2\partial\sigma^2} + \frac{\partial^4}{\partial\sigma^4}\right] \end{aligned}\right\} \tag{3.1.9}$$

and assume that the number of circumferential buckles is of such a magnitude that

$$\frac{n^3 h}{R} \sim O(1). \tag{3.1.10}$$

This assumption can be justified by experiment. The tests of Lundquist[7], Donnell[17], and Tennyson[31] show that, if only the final buckled shape is considered, for all of the cylinders tested $\frac{n^3 h}{R} \approx 1$ is a better choice than $\frac{n^2 h}{R} \approx 1$ (Appendix C). The assumption $\frac{n^2 h}{R} \approx 1$ can be used to show the consistancy of the Donnell equations for radial deflections of the order of the shell thickness (consistancy in the sense that all terms are of the same magnitude).

It is also noteworthy that the number of buckles decreases as buckling proceeds.

By the use of (3.1.2) through (3.1.9) Equations (2.24) can be written

$$\delta^2\gamma^2\bar{\nabla}^4 y + (\bar{P} - f_{,\sigma\sigma})y_{,\xi\xi} + 2f_{,\xi\sigma}y_{,\xi\sigma} - f_{,\xi\xi}(y_{,\sigma\sigma}+1) = 0$$

$$\delta^2\bar{\nabla}^4 f - y^2_{,\xi\sigma} + y_{,\xi\xi}(y_{,\sigma\sigma}+1) = 0. \qquad (3.1.11)$$

Equations (3.1.11) are the governing shell equations in non-dimensional form. If the order-of-magnitude assumptions which have been made are valid then all terms except those with coefficients δ^2 and $\delta^2\gamma^2$ are near one in magnitude. δ^2 and $\delta^2\gamma^2$ are significantly less than one. The terms in (3.1.11) which are multiplied by δ^2 and $\delta^2\gamma^2$ are those exhibiting the highest derivatives. This is typical of equations which describe problems for which a boundary layer type solution is expected.[32]

To solve Equation (3.1.11) consider only the region (012) and its boundaries. Take the solution to have the form

$$y = y_0 + y_1 + y_2 + y_3$$

$$f = f_0 + f_1 + f_2 + f_3 . \qquad (3.1.12)$$

The functions y_0 and f_0 describe the deflections and stresses in the field. The functions y_1 and f_1 describe the

additional deflection and stresses in the region including the valley (12) and are negligible in the rest of the region. Similarly y_2, f_2, y_3, and f_3 are functions which are nonnegligible only near ridges (02) and (01) respectively.

3.2. Solution Near a Valley

Consider first the solution near and including the valley (12). In this region the only nonnegligible functions are y_0, y_1, f_0, and f_1. The functions y_1 and f_1 are expanded in a power series in δ. Since y_1 and f_1 represent the boundary layer portion of the solution near (12) the independent coordinate normal to the valley is stretched to magnify the effect of the boundary layer. Then

$$\left.\begin{aligned} y &= y_0(\xi,\sigma) + \delta y_{11}(\psi,\sigma) + \delta^2 y_{12}(\psi,\sigma) + \cdots \\ f &= f_0(\xi,\sigma) + \delta f_{11}(\psi,\sigma) + \delta^2 f_{12}(\psi,\sigma) + \cdots \end{aligned}\right\} \qquad (3.2.1)$$

in which

$$\psi \equiv \frac{\xi}{\delta} \,. \qquad (3.2.2)$$

The functions y_0 and f_0 should be solutions to (3.1.11) with δ equal to zero, that is y_0 and f_0 should satisfy

$$\left.\begin{aligned} (\bar{P} - f_{0,\sigma\sigma})y_{0,\xi\xi} + 2f_{0,\xi\sigma}y_{0,\xi\sigma} + f_{0,\xi\xi}(y_{0,\sigma\sigma} + 1) &= 0 \\ y_{0,\xi\sigma}^2 - y_{0,\xi\xi}(y_{0,\sigma\sigma} + 1) &= 0 \,. \end{aligned}\right\} \qquad (3.2.3)$$

The original shape of the shell in terms of dimensionless variables is given by the expression

$$Y = -\alpha_3 + \tfrac{1}{2}\sigma^2 \tag{3.2.4}$$

The observed buckled shape seems to consist of a sequence of planes joined together at the ridges and valleys. However, equilibrium considerations (Appendix B) imply that some curvature in the circumferential direction is necessary. A null value for k also does not lead to boundary layer equations which have solutions which decay as the coordinate normal to the boundary increases. For these reasons the final shape in the field is assumed to retain some curvature in the σ direction and vary linearly with ξ, that is,

$$Y + y_0 = -\alpha_4 + \tfrac{1}{2}k\sigma^2 - 2(\alpha_2 + \alpha_3 - \alpha_4)\frac{l}{l_x}|\xi| \tag{3.2.5}$$

or

$$y_0 = (\alpha_3 - \alpha_4) - \tfrac{1}{2}(1-k)\sigma^2 - 2(\alpha_2 + \alpha_3 - \alpha_4)\frac{l}{l_x}|\xi| \ . \tag{3.2.6}$$

The initial stress state consists only of a compressive axial stress field equal in magnitude to the applied stress. In the buckled state the load may be expected to be carried also in the ridges and valleys, the ridges carrying compressive loads the valleys tensile loads. If this is the case for equilibrium in the radial direction along a valley, the stress in the field must be tensile. (Appendix B) Therefore let

$$f_o = (1+m)\frac{\bar{P}\sigma^2}{2} \tag{3.2.7}$$

in which m is an as yet unknown parameter such that $m = 0$ means that the total stress in the buckled state in the field vanishes.

The functions y_o and f_o as given in (3.2.6) and (3.2.7) satisfy Equations (3.2.3) except along the line $\xi = 0$.

Substituting (3.2.1) and (3.2.2) in (3.1.11) and collecting terms with like powers of δ as coefficients leads to the following sets of equations:

$$\left.\begin{aligned} &\gamma^2 y_{11,\psi\psi\psi\psi} - m\bar{P} y_{11,\psi\psi} - k f_{11,\psi\psi} = 0 \\ &f_{11,\psi\psi\psi\psi} + k y_{11,\psi\psi} = 0 \end{aligned}\right\} \tag{3.2.8}$$

$$\left.\begin{aligned} &\gamma^2 y_{12,\psi\psi\psi\psi} - m\bar{P} y_{12,\psi\psi} - k f_{12,\psi\psi} - f_{11,\sigma\sigma} y_{11,\psi\psi} \\ &\qquad + 2 f_{11,\psi\sigma} y_{11,\psi\sigma} - f_{11,\psi\psi} y_{11,\sigma\sigma} = 0 \\ &f_{12,\psi\psi\psi\psi} + k y_{12,\psi\psi} - y_{11,\psi\sigma}^2 + y_{11,\psi\psi} y_{11,\sigma\sigma} = 0 . \end{aligned}\right\} \tag{3.2.9}$$

The remaining sets of equations can be written down in a similar way. For a first approximation consider only

$$\left.\begin{aligned} y &= y_o + \delta y_{11} \\ f &= f_o + \delta f_{11} . \end{aligned}\right\} \tag{3.2.10}$$

The functions y_{11}, f_{11}, must be chosen to satisfy the symmetry and continuity conditions violated by y_o and f_o, and they should decay as $|\psi|$ increases. Therefore, y_{11} satisfies the following conditions:

$$\left.\begin{array}{ll} (Y + y_o + \delta y_{11}) \text{ continuous at } \xi = 0 \\ (Y + y_o + \delta y_{11})_{,\xi} = 0 \text{ at } \xi = 0 \\ (Y + y_o + \delta y_{11})_{,\xi\xi} \text{ continuous at } \xi = 0 \\ (Y + y_o + \delta y_{11})_{,\xi\xi\xi} = 0 \text{ at } \xi = 0 . \end{array}\right\} \quad (3.2.11)$$

In addition symmetry requires that

$$u_x(0,\sigma) = 0 \quad (3.2.12)$$

$$f_{,\xi}(0,\sigma) = 0 . \quad (3.2.13)$$

Since only ψ derivatives appear in Equation (3.2.8) and because of the observed buckled shape assume

$$\left.\begin{array}{l} y_{11} = y_{11}(\psi) \\ f_{11} = f_{11}(\psi) . \end{array}\right\} \quad (3.2.14)$$

Then the equations for y_{11} and f_{11} become

$$\gamma^2 \frac{d^4 y_{11}}{d\psi^4} - m\bar{P} \frac{d^2 y_{11}}{d\psi^2} - k \frac{d^2 f_{11}}{d\psi^2} = 0$$

$$\frac{d^4 f_{11}}{d\psi^4} + k \frac{d^2 y_{11}}{d\psi^2} = 0 . \qquad (3.2.15)$$

Two cases must be considered in solving (3.2.15) .

Case I

$$q_0^2 \equiv \frac{4\gamma^2 k^2}{m^2 \bar{P}^2} - 1 > 0 \qquad (3.2.16)$$

For this case the solution to (3.2.15) is (Appendix D)

$$\left.\begin{aligned} y_{11} &= b_1 e^{\lambda A_1 \psi} \cos \lambda A_2 \psi + b_2 e^{\lambda A_1 \psi} \sin \lambda A_2 \psi \\ f_{11} &= -\frac{m\bar{P}}{2k}\Big[(b_1 - q_0 b_2) e^{\lambda A_1 \psi} \cos \lambda A_2 \psi + (b_2 + q_0 b_1) e^{\lambda A_1 \psi} \sin \lambda A_2 \psi \\ &\quad + b_5 \psi\Big] \qquad (\psi < 0) \end{aligned}\right\} \qquad (3.2.17)$$

$$\left.\begin{aligned} y_{11} &= b_3 e^{-\lambda A_1 \psi} \cos \lambda A_2 \psi + b_4 e^{-\lambda A_1 \psi} \sin \lambda A_2 \psi \\ f_{11} &= -\frac{m\bar{P}}{2k}\Big[(b_3 + q_0 b_4) e^{-\lambda A_1 \psi} \cos \lambda A_2 \psi + (b_4 - q_0 b_3) e^{-\lambda A_1 \psi} \sin \lambda A_2 \psi \\ &\quad + b_6 \psi\Big] \qquad (\psi > 0) \end{aligned}\right\} \qquad (3.2.18)$$

in which

$$\left.\begin{aligned} A_1 &\equiv \sqrt{2}\,\cos\frac{\theta}{2} & A_2 &\equiv \sqrt{2}\,\sin\frac{\theta}{2} \\ \sin\theta &\equiv \frac{q}{\sqrt{1+q^2}} & \cos\theta &\equiv \frac{-1}{\sqrt{1+q^2}} \\ \lambda &\equiv \sqrt{\frac{k}{2\gamma}}. \end{aligned}\right\} \qquad (3.2.19)$$

The solutions to (3.2.15) given in (3.2.17) and (3.2.18) are chosen so that y_{11} and the boundary layer stresses decay as $|\psi|$ increases.

The use of (3.2.11) and (3.2.13) gives the following values for the constants in (3.2.17) and (3.2.18):

$$\left.\begin{aligned} b_1 = b_3 &= -\frac{(3A_1^2 - A_2^2)(\alpha_2+\alpha_3-\alpha_4)\ell}{2A_1\lambda\ell_x} \\ b_2 = -b_4 &= -\frac{(3A_2^2 - A_1^2)(\alpha_2+\alpha_3-\alpha_4)\ell}{2A_2\lambda\ell_x} \\ b_5 = -b_6 &= -\frac{2m\bar{P}(\alpha_2+\alpha_3-\alpha_4)\ell}{k\ell_x}. \end{aligned}\right\} \qquad (3.2.20)$$

Thus, to a first approximation,

$$y=(a_2-a_4)-\tfrac{1}{2}(1-k)\sigma^2-\frac{(a_2+a_3-a_4)}{l_x}\Big[2|\xi|+\frac{\delta}{2\lambda}e^{-\lambda A_1|\psi|}\Big(\frac{(3A_1^2-A_2^2)}{A_1}\cos\lambda A_2|\psi|-\frac{3A_2^2-A_1^2}{A_2}\sin\lambda A_2|\psi|\Big)\Big]$$

$$f=\tfrac{1}{2}(1+m)\bar{P}\sigma^2+\frac{m\bar{P}(a_2+a_3-a_4)\delta l}{4k\lambda l_x}\Big\{8\lambda|\psi|+e^{-\lambda A_1|\psi|}\Big[\Big(\frac{(3A_1^2-A_2^2)}{A_1}-q\frac{(3A_2^2-A_1^2)}{A_2}\Big)\cos\lambda A_2|\psi|-\Big(\frac{(3A_2^2-A_1^2)}{A_2}+\frac{(3A_1^2-A_2^2)}{A_1}\Big)\sin\lambda A_2|\psi|\Big]\Big\} \qquad (3.2.21)$$

or in terms of the original variables,

$$w=(a_3-a_4)-\frac{1}{2R}(1-k)s^2-\frac{(a_2+a_3-a_4)}{l_x}\Big[2|x|+\frac{\delta l}{2\lambda}e^{-\frac{\lambda A_1}{\delta l}|x|}\Big(\frac{(3A_1^2-A_2^2)}{A_1}\cos\frac{\lambda A_2}{\delta l}|x|-\frac{(3A_2^2-A_1^2)}{A_2}\sin\frac{\lambda A_2}{\delta l}|x|\Big)\Big]$$

$$F=\tfrac{1}{2}(1+m)Ps^2+\frac{mP(a_2+a_3-a_4)\delta l^3}{4k\lambda nh\, l_x}\Big\{8\frac{\lambda}{\delta l}|x|+e^{-\frac{\lambda A_1}{\delta l}|x|}\Big[\Big(\frac{(3A_1^2-A_2^2)}{A_1}-q\frac{(3A_2^2-A_1^2)}{A_2}\Big)\cos\frac{\lambda A_2}{\delta l}|x|-\Big(\frac{(3A_2^2-A_1^2)}{A_2}+q\frac{(3A_1^2-A_2^2)}{A_1}\Big)\sin\frac{\lambda A_2}{\delta l}|x|\Big]\Big\}. \qquad (3.2.22)$$

The additional stress are

$$\left.\begin{aligned} N_{xx} &= (1+m)P \\ N_{xs} &= 0 \\ N_{ss} &= \frac{mP(a_2+a_3-a_4)\lambda\ell}{\delta k n h \ell_x} e^{\frac{-\lambda A_1}{\delta\ell}|x|}\left[\left(\frac{1}{A_1}+\frac{9}{A_2}\right)\cos\frac{\lambda A_2}{\delta\ell}|x| + \left(\frac{1}{A_2}-\frac{9}{A_1}\right)\right. \\ &\quad \left.\sin\frac{\lambda A_2}{\delta\ell}|x|\right]. \end{aligned}\right\} \quad (3.2.23)$$

The axial and circumferential displacements can be calculated by solving Equations (2.15) for $u_{x,x}$, $u_{s,s}$ and $u_{x,s} + u_{s,x}$.

$$\left.\begin{aligned} u_{x,x} &= \frac{1}{Eh}(N_{xx}-\nu N_{ss}) - w_{,x}W_{,x} - \frac{1}{2}w_{,x}^2 \\ u_{s,s} &= \frac{1}{Eh}(N_{ss}-\nu N_{xx}) - w_{,s}W_{,s} - \frac{1}{2}w_{,s}^2 \\ u_{x,s}+u_{s,x} &= \frac{2(1+\nu)}{Eh}N_{xs} - w_{,x}w_{,s} - w_{,x}W_{,s} - w_{,s}W_{,x} \end{aligned}\right\} \quad (3.2.24)$$

Since the compatibility of the strains and displacements has been assured, Equations (3.2.24) can be integrated by using the results of Equations (3.2.23), (3.2.22) and (2.21). The constants of integration can be found by making N_{xs} , as calculated from Equation (2.15), be zero, and then satisfying condition (3.2.12). It is noted that this condition can be satisfied only in the average; hence the solution is approximate. The expressions for u_x and u_s are

$$u_x(x>0) = \frac{(1+m)}{Eh} p - \frac{2\nu m P(a_2+a_3-a_4)\ell^2}{nEh^2 k \ell_x}\left[1 - e^{\frac{-\lambda A_1}{\delta\ell}x}\left(\cos\frac{\lambda A_2}{\delta\ell}x - \left(\frac{\delta}{2}-\frac{1}{2\delta}\right)\sin\frac{\lambda A_2}{\delta\ell}x\right)\right] + \frac{2(a_2+a_3-a_4)^2}{\ell_x^2}\left\{x + \frac{\delta\ell}{2\lambda}e^{\frac{-\lambda A_1}{\delta\ell}x}\left[\frac{(3A_1^2-A_2^2)}{A_1}\cos\frac{\lambda A_2}{\delta\ell}x - \frac{(3A_2^2-A_1^2)}{A_2}\sin\frac{\lambda A_2}{\delta\ell}x\right] + \frac{\delta\ell}{2\lambda}e^{\frac{-2\lambda A_1}{\delta\ell}x}\left[\left(A_2 - \frac{2A_1}{\delta} - \frac{A_2}{\delta^2}\right)\sin\frac{2\lambda A_2}{\delta\ell}x - \left(A_1 + \frac{2A_2}{\delta} - \frac{A_1}{\delta^2}\right)\cos\frac{2\lambda A_2}{\delta\ell}x - \frac{2}{A_1}\left(1+\frac{1}{\delta}\right)\right] - \frac{\delta\ell}{2\lambda}\left[\frac{(3A_1^2-A_2^2)}{A_1} - \frac{1}{4}\left(A_1 + \frac{2A_2}{\delta} - \frac{A_1}{\delta^2}\right) - \frac{1}{2A_1}\left(1+\frac{1}{\delta}\right)\right]\right\} + \frac{k(a_2+a_3-a_4)}{R\ell_x}\left(s^2 - \frac{\ell_s^2}{12}\right) \qquad (3.2.25)$$

$$u_x(x<0) = -u_x(x>0)$$

$$u_s = -\frac{\nu(1+m)}{Eh} p_s + \frac{mP(a_2+a_3-a_4)\lambda\ell}{\delta nEh^2 k \ell_x} e^{\frac{-\lambda A_1}{\delta\ell}|x|}\left[\left(\frac{1}{A_1}+\frac{\delta}{A_2}\right)\cos\frac{\lambda A_2}{\delta\ell}|x| + \left(\frac{1}{A_2}-\frac{\delta}{A_1}\right)\sin\frac{\lambda A_2}{\delta\ell}|x|\right]s + \frac{(1-k^2)s^3}{6k^2}.$$

Case II

$$q^2 < 0 \tag{3.2.26}$$

With the introduction of

$$\left.\begin{aligned} p^2 &\equiv 1 - \frac{4\gamma^2 k^2}{m^2 \bar{P}^2} = -q^2 \\ A_3 &\equiv \sqrt{\frac{m\bar{P}}{k\gamma}}\sqrt{1+p} \\ A_4 &\equiv \sqrt{\frac{m\bar{P}}{k\gamma}}\sqrt{1-p} \\ \lambda &\equiv \sqrt{\frac{k}{2\gamma}} \end{aligned}\right\} \tag{3.2.27}$$

the solution to Equation (3.2.15) corresponding to (3.2.17) and (3.2.18) is

$$\left.\begin{aligned} y_{11} &= b_7 e^{\lambda A_3 \psi} + b_8 e^{\lambda A_4 \psi} \\ f_{11} &= -\frac{m\bar{P}}{2k}\left[b_7 A_4^2 e^{\lambda A_3 \psi} + b_8 A_3^2 e^{\lambda A_4 \psi} + b_{11}\psi\right] \\ \psi &< 0 \end{aligned}\right\} \tag{3.2.28}$$

$$\left.\begin{aligned} y_{11} &= b_9 e^{-\lambda A_3 \psi} + b_{10} e^{-\lambda A_4 \psi} \\ f_{11} &= -\frac{m\bar{P}}{2k}\left[b_9 A_4^2 e^{-\lambda A_3 \psi} + b_{10} A_3^2 e^{-\lambda A_4 \psi} + b_{12}\psi\right] \\ \psi &> 0 . \end{aligned}\right\} \tag{3.2.29}$$

The use of the continuity conditions at $\psi = 0$ gives the following values for the constants in (3.2.28) and (3.2.29):

$$\left.\begin{aligned} b_7 = b_9 &= \frac{2A_4^2(\alpha_2+\alpha_3-\alpha_4)\ell}{A_3(A_3^2-A_4^2)\lambda\ell_x} \\ b_8 = b_{10} &= -\frac{2A_3^2(\alpha_2+\alpha_3-\alpha_4)\ell}{A_4(A_3^2-A_4^2)\lambda\ell_x} \\ b_{11} = b_{12} &= \frac{-4(\alpha_2+\alpha_3-\alpha_4)\ell}{\ell_x} \end{aligned}\right\} \qquad (3.2.30)$$

Thus

$$\left.\begin{aligned} y &= (\alpha_3-\alpha_4)-\tfrac{1}{2}(1-k)\sigma^2-\frac{2(\alpha_2+\alpha_3-\alpha_4)\ell}{\ell_x}\Big[|\xi| \\ &\quad -\frac{\delta A_4^2}{\lambda A_3(A_3^2-A_4^2)}e^{-\lambda A_3|\psi|}+\frac{\delta A_3^2}{\lambda A_4(A_3^2-A_4^2)}e^{-\lambda A_4|\psi|}\Big] \\ f &= \tfrac{1}{2}(1+m)\bar{P}\sigma^2+\frac{\delta m\bar{P}(\alpha_2+\alpha_3-\alpha_4)\ell}{\lambda k\ell_x}\Big[2\lambda|\psi| \\ &\quad -\frac{A_4^4}{A_3(A_3^2-A_4^2)}e^{-\lambda A_3|\psi|}+\frac{A_3^4}{A_4(A_3^2-A_4^2)}e^{-\lambda A_4|\psi|}\Big] \end{aligned}\right\} \qquad (3.2.31)$$

or in terms of the original variables

$$w = (a_3-a_4) - \frac{1}{2R}(1-k)s^2 - \frac{2(a_2+a_3-a_4)}{l_x}\Big[|x| - \frac{\delta l A_4^2}{\lambda A_3(A_3^2-A_4^2)} e^{-\frac{\lambda A_3}{\delta l}|x|} + \frac{\delta l A_3^2}{\lambda A_4(A_3^2-A_4^2)} e^{-\frac{\lambda A_4}{\delta l}|x|}\Big]$$

$$F = \frac{1}{2}(1+m)Ps^2 + \frac{\delta m P(a_2+a_3-a_4)l^3}{\lambda k n h l_x}\Big[\frac{2\lambda}{\delta l}|x| - \frac{A_4^4}{A_3(A_3^2-A_4^2)} e^{-\frac{\lambda A_3}{\delta l}|x|} + \frac{A_3^4}{A_4(A_3^2-A_4^2)} e^{-\frac{\lambda A_4}{\delta l}|x|}\Big]. \qquad (3.2.32)$$

The additional stresses are

$$N_{xx} = (1+m)P$$

$$N_{xs} = 0$$

$$N_{ss} = \frac{\lambda m P(a_2+a_3-a_4)l^2}{nEh^2 k l_x}\Big[\frac{A_4 A_3^4}{A_3^2-A_4^2} e^{-\frac{\lambda A_4}{\delta l}|x|} - \frac{A_3 A_4^4}{A_3^2-A_4^2} e^{-\frac{\lambda A_3}{\delta l}|x|}\Big]. \qquad (3.2.33)$$

The displacements in the x and s directions are

$$u_x(x>0) = \frac{(1+m)P}{Eh}x + \frac{\nu m P(a_2+a_3-a_4)\ell^2}{nEh^2 k l_x}\left[\frac{A_3^4}{A_3^2-A_4^2}e^{\frac{-\lambda A_4}{\delta\ell}x}\right.$$

$$\left.-\frac{A_4^4}{A_3^2-A_4^2}e^{\frac{-\lambda A_3}{\delta\ell}x}-2\right]-\frac{4(a_2+a_3-a_4)^2\delta\ell}{\lambda l_x^2}\left\{\frac{\lambda x}{2\delta\ell}\right.$$

$$+\frac{A_4^2}{A_3(A_3^2-A_4^2)}\left(1-e^{\frac{-\lambda A_3}{\delta\ell}x}\right)-\frac{A_3^2}{A_4(A_3^2-A_4^2)}\left(1-e^{\frac{-\lambda A_4}{\delta\ell}x}\right)$$

$$-\frac{A_3^2A_4^2}{(A_3+A_4)(A_3^2-A_4^2)^2}\left(1-e^{\frac{-\lambda(A_3+A_4)}{\delta\ell}x}\right)+\frac{A_4^4}{4A_3(A_3^2-A_4^2)^2}$$

$$\left.\left(1-e^{\frac{-2\lambda A_3}{\delta\ell}x}\right)+\frac{A_3^4}{4A_4(A_3^2-A_4^2)^2}\left(1-e^{\frac{-2\lambda A_4}{\delta\ell}x}\right)\right\} \qquad (3.2.34)$$

$$+\frac{k(a_2+a_3-a_4)}{Rl_x}\left(s^2-\frac{l_s^2}{12}\right)$$

$$u_x(x<0) = -u_x(x>0)$$

$$u_s = -\frac{\nu(1+m)P}{Eh}s + \frac{\lambda m P(a_2+a_3-a_4)\ell}{\delta nEh^2 k l_x}\left[\frac{A_4A_3^4}{A_3^2-A_4^2}e^{\frac{-\lambda A_4}{\delta\ell}|x|}\right.$$

$$\left.-\frac{A_3A_4^4}{A_3^2-A_4^2}e^{\frac{-\lambda A_3}{\delta\ell}|x|}\right]s+\frac{(1-k^2)}{6R^2}s^3.$$

3.3. Solution Near a Ridge

Consider the solution to (3.1.11) near the ridge (02). Because of the symmetry of the buckled shape, the solution for this ridge suitably modified is valid for all other ridges.

To consider the ridge (02), a new reference plane, Π_2, and a new coordinate system are chosen. The coordinate system is selected to lie in a plane containing a straight line joining the points (0) and (2) in the buckled state and orthogonal to a radius of the unbuckled cylinder at the midpoint of the line (02). The co ordinates used to describe the solution are taken to lie in Π_2 in the directions along the ridges (01) and (02). (Figure 3.1.)

This new reference plane, Π_2, does not change the form of the basic equations[33], but the displacement functions are now taken with respect to Π_2. This change is possible since the number of circumferential buckles is large and therefore the angle $\frac{\pi}{n}$ is such that $\frac{\pi^2}{n^2} \ll 1$. The slope of Π_2 with respect to Π_1 is $\frac{\pi}{2n}$. This is a sufficient condition that the form of the equations be the same.

The governing equations are rewritten denoting the new dependent variables by primes and the new independent variables by a bar whenever confusion might arise. They are

$$\left.\begin{aligned} &D\nabla^4 w' + P w'_{,\bar{x}\bar{x}} - F'_{,\bar{s}\bar{s}}(w'+W')_{,\bar{x}\bar{x}} + 2F'_{,\bar{x}\bar{s}}(w'+W')_{,\bar{x}\bar{s}} - F_{,xx}(w'+W')_{,\bar{s}\bar{s}} = 0 \\ &\nabla^4 F' - Eh\left(w'^2_{,\bar{x}\bar{s}} - w'_{,\bar{x}\bar{x}} w'_{,\bar{s}\bar{s}} + 2w'_{,\bar{x}\bar{s}} W'_{,\bar{x}\bar{s}} - w'_{,\bar{x}\bar{x}} W'_{,\bar{s}\bar{s}} - w'_{,\bar{s}\bar{s}} W'_{,\bar{x}\bar{x}}\right) = 0. \end{aligned}\right\} \quad (3.3.1)$$

The initial stress, P, is the same in either Π_1 or Π_2. The coordinates $\bar{x}$ and $\bar{s}$ are the projections of x and s on Π_2. $\bar{x}$ is an axial coordinate and $\bar{s}$ a circumferential one.

Again (3.3.1) is put in nondimensional form by using the following transformations:

$$\left.\begin{aligned} W' &\equiv nhY' \\ w' &\equiv nhy' \\ P &\equiv \frac{nEh}{l^2}\bar{P} \\ F' &\equiv nEh^3 f' \end{aligned}\right\} \qquad (3.3.2)$$

$$\left.\begin{aligned} \varsigma &\equiv \frac{\bar{X}}{l_x} - \frac{\bar{S}}{l_s} + \frac{1}{2} \\ \varrho &\equiv \frac{\bar{X}}{l_x} + \frac{\bar{S}}{l_s} + \frac{1}{2} \\ \bar{S} &\equiv \frac{l_s}{2}(\varrho - \varsigma) \\ \bar{X} &\equiv \frac{l_x}{2}(\varrho + \varsigma - 1) \end{aligned}\right\} \qquad (3.3.3)$$

The nondimensional equations are

$$\left.\begin{aligned}
&\delta^2\gamma^2\bar{\bar{\nabla}}^4 Y' + \frac{\nu^2 \ell_s^2}{\ell^2}\bar{P}\left(Y'_{,\rho\rho} + 2Y'_{,\rho\varsigma} + Y'_{,\varsigma\varsigma}\right) - 4\nu^2\left[f'_{,\rho\rho}\left(Y'+\bar{Y}'\right)_{,\varsigma\varsigma}\right. \\
&\left. -2f'_{,\rho\varsigma}\left(Y'+\bar{Y}'\right)_{,\rho\varsigma} + f'_{,\varsigma\varsigma}\left(Y'+\bar{Y}'\right)_{,\rho\rho}\right] = 0 \\
&\delta^2\bar{\bar{\nabla}}^4 f' - 4\nu^2\left(Y'^2_{,\rho\varsigma} - Y'_{,\rho\rho}Y'_{,\varsigma\varsigma} + 2Y'_{,\rho\varsigma}\bar{Y}'_{,\rho\varsigma} - Y'_{,\rho\rho}\bar{Y}'_{,\varsigma\varsigma}\right. \\
&\left. - Y'_{,\varsigma\varsigma}\bar{Y}'_{,\rho\rho}\right) = 0
\end{aligned}\right\} \quad (3.3.4)$$

in which

$$\left.\begin{aligned}
\bar{\bar{\nabla}}^4 \equiv \Big[&(1+\nu^2)^2\left(\frac{\partial^4}{\partial\rho^4} + \frac{\partial^4}{\partial\varsigma^4}\right) - 4(1-\nu^4)\left(\frac{\partial^4}{\partial\rho\partial\varsigma^3} + \frac{\partial^4}{\partial\rho^3\partial\varsigma}\right) \\
&+ 2(3-2\nu^2+3\nu^4)\frac{\partial^4}{\partial\rho^2\partial\varsigma^2}\Big].
\end{aligned}\right\} \quad (3.3.5)$$

The coordinate system ρ , ζ is oriented as shown in Figure 3.2. It should be noted that the coordinates ρ and ζ are orthogonal only in the special case $\mu = 1$.

The original shape of the cylinder is again approximated by the parabola

$$\bar{Y}' = a_2 - 4a_5(\rho - \varsigma) + 4a_5(\rho - \varsigma)^2 \qquad (3.3.6)$$

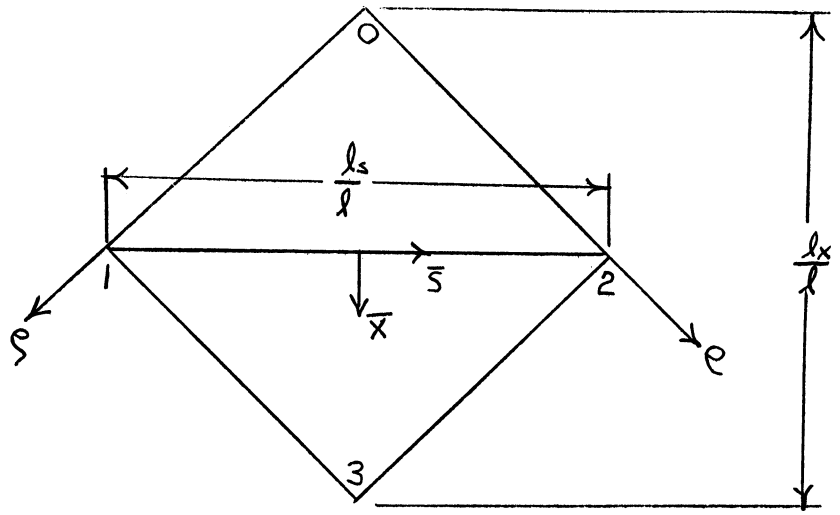

Figure 3.2. Orientation of the ρ , ζ Coordinate System.

in which

$$\alpha_5 \equiv \frac{a_5}{nh} \qquad a_5 \approx \frac{\pi^2 R}{8n^2}. \qquad \text{(Appendix A)} \qquad (3.3.7)$$

By the use of (3.3.3), Equations (3.3.4) become

$$\left.\begin{aligned} &\delta^2\gamma^2\bar{\bar{\nabla}}^4 Y' + \frac{\nu^2 l_s^2}{l^2}\bar{P}(Y'_{,ee} + 2Y'_{,e\zeta} + Y'_{,\zeta\zeta}) - 32\nu^3\alpha_5(f'_{,ee} \\ &+ 2f'_{,e\zeta} + f'_{,\zeta\zeta}) - 4\nu^2(f'_{,ee}Y'_{,\zeta\zeta} - 2f'_{,e\zeta}Y'_{,e\zeta} + f'_{,\zeta\zeta}Y'_{,ee}) \\ &= 0 \end{aligned}\right\} \quad (3.3.8)$$

$$\delta^2\bar{\bar{\nabla}}^4 f' - 4\nu^2\left[Y'^2_{,e\zeta} - Y'_{,ee}Y'_{,\zeta\zeta} - 8\alpha_5(Y'_{,ee} + 2Y'_{,e\zeta} + Y'_{,\zeta\zeta})\right] = 0.$$

As in the solution for the region including the valley (12) the functions y' and f' are taken to be the sum of two terms, the first term being the solution in the field and the other representing the boundary layer. The boundary layer term is expanded in a power series in δ and the independent variable ζ is stretched to magnify the effect of the boundary layer. Let

$$y' = y_0'(\rho,\varsigma) + \delta y_{21}(\rho,\eta) + \delta^2 y_{22}(\rho,\eta) + \cdots$$
$$f' = f_0'(\rho,\varsigma) + \delta f_{21}(\rho,\eta) + \delta^2 f_{22}(\rho,\eta) + \cdots \qquad (3.3.9)$$

in which

$$\eta \equiv \frac{\varsigma}{\delta} \qquad (3.3.19)$$

The functions y_0' and f_0' correspond to y_0 and f_0; they differ in that y_0' and f_0' are taken with respect to Π_2. y_0' and f_0' satisfy (3.3.8) with $\delta = 0$, in view of the preceding results this implies

$$\left.\begin{aligned} y_0' &= -\alpha_2 + (\alpha_2+\alpha_3-\alpha_4)(\rho+\varsigma) - (\alpha_2+\alpha_3-4\alpha_5)(\rho-\varsigma) \\ &\quad + (\alpha_4-4\alpha_5)(\rho-\varsigma)^2 \qquad (\varsigma>0) \\ y_0' &= -\alpha_2 - (\alpha_2+\alpha_3-\alpha_4)(\rho+\varsigma) + (\alpha_2+\alpha_3-2\alpha_4+4\alpha_5)(\rho-\varsigma) \\ &\quad + (\alpha_4-4\alpha_5)(\rho-\varsigma)^2 \qquad (\varsigma<0) \\ f_0' &= (1+m)\frac{P l_s^2}{l^2}(\rho-\varsigma)^2 \end{aligned}\right\} \qquad (3.3.11)$$

Substituting (3.3.9) and (3.1.11) in (3.3.8) and collecting terms with like powers of δ as coefficients leads to the following sets of equations (only the first two sets of equations are given):

$$\left.\begin{aligned} &\gamma^2 y_{21,\eta\eta\eta\eta} - \bar{m}\bar{P} y_{21,\eta\eta} - \bar{k} f_{21,\eta\eta} = 0 \\ &f_{21,\eta\eta\eta\eta} + \bar{k} y_{21,\eta\eta} = 0 \end{aligned}\right\} \tag{3.3.12}$$

$$\left.\begin{aligned} &\gamma^2 y_{22,\eta\eta\eta\eta} - \bar{m}\bar{P} y_{22,\eta\eta} - k f_{22,\eta\eta} - 4\gamma^2 \frac{(1-\nu^2)}{(1+\nu^2)} y_{21,e\eta\eta\eta} \\ &\quad + \frac{2\nu^2 l_s^2}{(1+\nu^2)^2 l^2} \bar{P} y_{21,e\eta} - \frac{64\nu^2 \alpha_5}{(1+\nu^2)^2} f_{21,e\eta} - \frac{1}{(1+\nu^2)^2}\Big(\\ &\quad 2 f_{21,e\eta} y_{21,e\eta} + f_{21,ee} y_{21,\eta\eta} + f_{21,\eta\eta} y_{21,ee} \Big) = 0 \\ &f_{22,\eta\eta\eta\eta} + \bar{k} y_{22,\eta\eta} - 4\gamma^2 \frac{(1-\nu^2)}{(1+\nu^2)} f_{21,e\eta\eta\eta} - \frac{64\nu^2 \alpha_5}{(1+\nu^2)^2} y_{21,e\eta} \\ &\quad + \frac{4\nu^2}{(1+\nu^2)^2}\left(y_{21,e\eta}^2 - y_{21,ee} y_{21,\eta\eta} \right) = 0 \end{aligned}\right\} \tag{3.3.13}$$

in which

$$\left.\begin{aligned} \bar{m} &\equiv \frac{\nu^2 l_s^2 m}{(1+\nu^2)^2 l^2} \\ \bar{k} &\equiv \frac{8\nu^2 \alpha_4}{(1+\nu^2)^2} . \end{aligned}\right\} \tag{3.3.14}$$

It is easily shown (Appendix A) that

$$\frac{\bar{m}}{\bar{k}} = \frac{m}{k}. \tag{3.3.15}$$

Again as in the solution for the valley (12), as a first approximation, take only the first two terms in (3.3.9), and let y_{21} and f_{21} be functions only of η, that is

$$\left.\begin{aligned} y' &= y_0' + \delta y_{21}(\eta) \\ f' &= f_0' + \delta f_{21}(\eta). \end{aligned}\right\} \tag{3.3.16}$$

The governing equations for y_{21} and f_{21} thus become

$$\left.\begin{aligned} \gamma^2 \frac{d^4 y_{21}}{d\eta^4} - \bar{m}\bar{p}\frac{d^2 y_{21}}{d\eta^2} - \bar{k}\frac{d^2 f_{21}}{d\eta^2} &= 0 \\ \frac{d^4 f_{21}}{d\eta^4} + \bar{k}\frac{d^2 y_{21}}{d\eta^2} &= 0. \end{aligned}\right\} \tag{3.3.17}$$

Because of the similarity between (3.3.17) and (3.2.15), a solution of (3.3.17) is

Case I

$$q^2 \equiv \frac{4\gamma^2 k^2}{m^2 \bar{p}^2} - 1 \quad > 0 \tag{3.3.18}$$

$$
\left.
\begin{aligned}
y_{21} &= b_{13} e^{\bar{\lambda} A_1 \eta} \cos \bar{\lambda} A_2 \eta + b_{14} e^{\bar{\lambda} A_1 \eta} \sin \bar{\lambda} A_2 \eta \\
f_{21} &= -\frac{m\bar{p}}{2k}\Big[(b_{13} - q_0 b_{14}) e^{\bar{\lambda} A_1 \eta} \cos \bar{\lambda} A_2 \eta + (b_{14} + q_0 b_{13}) \\
&\qquad e^{\bar{\lambda} A_1 \eta} \sin \bar{\lambda} A_2 \eta + b_{17} \eta\Big]
\end{aligned}
\right\} \quad (3.3.19)
$$

$\eta < 0$

$$
\left.
\begin{aligned}
y_{21} &= b_{15} e^{-\bar{\lambda} A_1 \eta} \cos \bar{\lambda} A_2 \eta + b_{16} e^{-\bar{\lambda} A_1 \eta} \sin \bar{\lambda} A_2 \eta \\
f_{21} &= \frac{m\bar{p}}{2k}\Big[(b_{15} + q_0 b_{16}) e^{-\bar{\lambda} A_1 \eta} \cos \bar{\lambda} A_2 \eta + (b_{16} - q_0 b_{15}) \\
&\qquad e^{-\bar{\lambda} A_1 \eta} \sin \bar{\lambda} A_2 \eta + b_{18} \eta\Big]
\end{aligned}
\right\} \quad (3.3.20)
$$

$\eta > 0$

in which

$$
\left.
\begin{aligned}
A_1 &\equiv \sqrt{2} \cos \frac{\theta}{2} & A_2 &\equiv \sqrt{2} \sin \frac{\theta}{2} \\
\cos \theta &\equiv \frac{1}{\sqrt{1+q_0^2}} & \sin \theta &\equiv \frac{q_0}{\sqrt{1+q_0^2}} \\
\bar{\lambda} &\equiv \sqrt{\frac{k}{2\gamma}} .
\end{aligned}
\right\} \quad (3.3.21)
$$

The continuity and symmetry conditions at the ridge are

$$\left.\begin{aligned} &(Y'+Y') \quad \text{continuous at} \quad \zeta = 0 \\ &(Y'+Y')_{,\bar{x}} = 0 \quad \text{at} \quad \zeta = 0 \\ &(Y'+Y')_{,\bar{x}\bar{x}} \quad \text{continuous at} \quad \zeta = 0 \\ &(Y'+Y')_{,\bar{x}\bar{x}\bar{x}} = 0 \quad \text{at} \quad \zeta = 0 \end{aligned}\right\} \tag{3.3.22}$$

$$f'_{,\bar{x}} = 0 \quad \text{at} \quad \zeta = 0 \,. \tag{3.3.23}$$

The use of (3.3.22) and (3.3.33) to find the unknown constants in (3.3.19) and (3.3.20) leads to

$$\left.\begin{aligned} b_{13} = b_{15} &= \frac{(3A_1^2 - A_2^2)(\alpha_2+\alpha_3-\alpha_4)}{2A_1\bar{\lambda}} \\ b_{14} = -b_{16} &= \frac{(3A_2^2 - A_1^2)(\alpha_2+\alpha_3-\alpha_4)}{2A_2\bar{\lambda}} \\ b_{17} = -b_{18} &= 4(\alpha_2+\alpha_3-\alpha_4) \end{aligned}\right\} \tag{3.3.24}$$

Thus

$$y_{21} = \frac{(\alpha_2+\alpha_3-\alpha_4)}{2\bar{\lambda}} e^{-\bar{\lambda}A_1|\eta|}\left[\frac{(3A_1^2-A_2^2)}{A_1}\cos\bar{\lambda}A_2|\eta| - \frac{(3A_2^2-A_1^2)}{A_2}\sin\bar{\lambda}A_2|\eta|\right]$$

$$f_{21} = \frac{-m\bar{P}(\alpha_2+\alpha_3-\alpha_4)}{4k\bar{\lambda}}\left\{8\bar{\lambda}|\eta| + e^{-\bar{\lambda}A_1|\eta|}\left[\left(\frac{(3A_1^2-A_2^2)}{A_1}\right.\right.\right.$$

$$\left.\left.\left. -q\frac{(3A_2^2-A_1^2)}{A_2}\right)\cos\bar{\lambda}A_2|\eta| - \left(\frac{(3A_2^2-A_1^2)}{A_2} + q\frac{(3A_1^2-A_2^2)}{A_1}\right)\sin\bar{\lambda}A_2|\eta|\right]\right\}. \qquad (3.3.25)$$

The functions y' and f' are

$$y' = -\alpha_2 + (\alpha_2+\alpha_3-\alpha_4)(\rho+\xi) - (\alpha_2+\alpha_3-4\alpha_5)(\rho-\xi)$$

$$+(\alpha_4-4\alpha_5)(\rho-\xi)^2 + \frac{8(\alpha_2+\alpha_3-\alpha_4)}{2\bar{\lambda}} e^{-\bar{\lambda}A_1\eta}\left[\frac{(3A_1^2-A_2^2)}{A_1}\right. \qquad (3.3.26)$$

$$\left.\cos\bar{\lambda}A_2\eta - \frac{(3A_2^2-A_1^2)}{A_2}\sin\bar{\lambda}A_2\eta\right] \qquad (\xi>0)$$

$$y' = -\alpha_2 - (\alpha_2+\alpha_3-\alpha_4)(\rho+\xi) + (\alpha_2+\alpha_3-2\alpha_4+4\alpha_5)(\rho-\xi)$$

$$+(\alpha_4-4\alpha_5)(\rho-\xi)^2 + \frac{8(\alpha_2+\alpha_3-\alpha_4)}{2\bar{\lambda}} e^{\bar{\lambda}A_1\eta}\left[\frac{(3A_1^2-A_2^2)}{A_1}\right. \qquad (3.3.27)$$

$$\left.\cos\bar{\lambda}A_2\eta + \frac{(3A_2^2-A_1^2)}{A_2}\sin\bar{\lambda}A_1\eta\right]. \qquad (\xi<0)$$

$$f' = \frac{(1+m)\bar{P}\ell_s^2}{8\ell^2}(\rho-\varsigma)^2 - \frac{\delta m(a_2+a_3-a_4)}{4k\bar{\lambda}}\Big\{8\bar{\lambda}|\eta| + e^{-\bar{\lambda}A_1|\eta|}\Big[\Big(\frac{(3A_1^2-A_2^2)}{A_1} - q\frac{(3A_2^2-A_1^2)}{A_2}\Big)\cos\bar{\lambda}A_2|\eta| - \Big(\frac{(3A_2^2-A_1^2)}{A_2} + q\frac{(3A_1^2-A_2^2)}{A_1}\Big)\sin\bar{\lambda}A_2|\eta|\Big]\Big\}. \qquad (3.3.28)$$

Equations (3.3.26), (3.3.27), and (3.3.28) can be written in terms of the original variables as follows:

$$w' = -a_2 - 2(a_2+a_3-a_4)(1+\frac{\bar{x}}{\ell_x}) + 2(a_2+a_3-2a_4+4a_5)\frac{\bar{s}}{\ell_s} + 4(a_4-a_5)\frac{\bar{s}^2}{\ell_s^2} + \frac{\delta(a_2+a_3-a_4)}{2\bar{\lambda}}e^{-\frac{\bar{\lambda}A_1\rho}{\delta}}\Big[\frac{(3A_1^2-A_2^2)}{A_1}\cos\frac{\bar{\lambda}A_2}{\delta}\varsigma + \frac{(3A_2^2-A_1^2)}{A_2}\sin\frac{\bar{\lambda}A_2}{\delta}\varsigma\Big]$$

$$F' = \frac{(1+m)\bar{P}}{2}\bar{s}^2 + \frac{\delta(a_2+a_3-a_4)\ell^2}{4k\bar{\lambda}nh}\Big\{\frac{8\bar{\lambda}}{\delta}\varsigma - e^{-\frac{\bar{\lambda}A_1}{\delta}\varsigma}\Big[\Big(\frac{(3A_1^2-A_2^2)}{A_1} - q\frac{(3A_2^2-A_1^2)}{A_2}\Big)\cos\frac{\bar{\lambda}A_2}{\delta}\varsigma - \Big(\frac{(3A_2^2-A_1^2)}{A_2} + q\frac{(3A_1^2-A_2^2)}{A_1}\Big)\sin\frac{\bar{\lambda}A_2}{\delta}\varsigma\Big]\Big\} \qquad (3.3.29)$$

$\varsigma > 0$.

$$w' = -a_2 + 2(a_2+a_3-a_4)(1+\frac{\bar{x}}{l_x}) - 2(a_2+a_3-4a_5)\frac{\bar{s}}{l_s} + 4(a_4-a_5)\frac{\bar{s}^2}{l_s^2}$$

$$+ \frac{\delta(a_2+a_3-a_4)}{2\bar{\lambda}} e^{\frac{\bar{\lambda}A_1}{\delta}\varsigma}\left[\frac{(3A_1^2-A_2^2)}{A_1}\cos\frac{\bar{\lambda}A_2}{\delta}\varsigma + \frac{(3A_2^2-A_1^2)}{A_2}\sin\frac{\bar{\lambda}A_2}{\delta}\varsigma\right]$$

$$F' = \frac{(1+m)P s^2}{2} + \frac{\delta m P(a_2+a_3-a_4)l^2}{4k\bar{\lambda}nh}\left\{\frac{\delta}{\bar{\lambda}}\varsigma - e^{\frac{\bar{\lambda}A_1}{\delta}\varsigma}\left[\right.\right. \tag{3.3.30}$$

$$\left(\frac{(3A_1^2-A_2^2)}{A_1} - q\frac{(3A_2^2-A_1^2)}{A_2}\right)\cos\frac{\bar{\lambda}A_2}{\delta}\varsigma + \left(\frac{(3A_2^2-A_1^2)}{A_2}\right.$$

$$\left.\left. + q\frac{(3A_1^2-A_2^2)}{A_1}\right)\sin\frac{\bar{\lambda}A_1}{\delta}\varsigma\right]\Big\}$$

$$\varsigma < 0$$

The stresses are found again by differentiating the stress function, namely,

$$N'_{\bar{x}\bar{x}} = F'_{,\bar{s}\bar{s}} = (1+m)P - \frac{mP(a_2+a_3-a_4)\bar{\lambda}l^2}{\delta k l_s^2 nh} e^{-\frac{\bar{\lambda}A_1}{\delta}|\varsigma|}\left[\left(\frac{1}{A_1}+\frac{q}{A_2}\right)\right. \tag{3.3.31}$$

$$\left.\cos\frac{\bar{\lambda}A_2}{\delta}|\varsigma| + \left(\frac{1}{A_2}-\frac{q}{A_1}\right)\sin\frac{\bar{\lambda}A_2}{\delta}|\varsigma|\right]$$

$$N'_{\bar{x}\bar{s}} = -F'_{,\bar{x}\bar{s}} = -\frac{mP(a_2+a_3-a_4)\bar{\lambda}\ell^2}{\delta k \ell_x \ell_s nh} e^{-\frac{\bar{\lambda}A_1}{\delta}|\varsigma|}\left[\left(\frac{1}{A_1}+\frac{q}{A_2}\right)\right.$$

$$\left.\cos\frac{\bar{\lambda}A_2}{\delta}|\varsigma| + \left(\frac{1}{A_2}-\frac{q}{A_1}\right)\sin\frac{\bar{\lambda}A_2}{\delta}|\varsigma|\right]$$

$$N'_{\bar{s}\bar{s}} = F'_{,\bar{x}\bar{x}} = -\frac{mP(a_2+a_3-a_4)\bar{\lambda}\ell^2}{\delta k \ell_x^2 nh} e^{-\frac{\bar{\lambda}A_1}{\delta}|\varsigma|}\left[\left(\frac{1}{A_1}+\frac{q}{A_2}\right)\right.$$

$$\left.\cos\frac{\bar{\lambda}A_2}{\delta}|\varsigma| + \left(\frac{1}{A_2}-\frac{q}{A_1}\right)\sin\frac{\bar{\lambda}A_2}{\delta}|\varsigma|\right] . \qquad (3.3.31)$$

The components of the additional stress in the ρ and ζ directions are also of interest. They are

$$N'_{\rho\rho} = \frac{\nu^2(1+m)P}{(1+\nu^2)} - \frac{(1+\nu^2)mP(a_2+a_3-a_4)\bar{\lambda}\ell^2}{\delta\nu k \ell_x \ell_s nh} e^{-\frac{\bar{\lambda}A_1}{\delta}|\varsigma|}$$

$$\left[\left(\frac{1}{A_1}+\frac{q}{A_2}\right)\cos\frac{\bar{\lambda}A_2}{\delta}|\varsigma| + \left(\frac{1}{A_2}-\frac{q}{A_1}\right)\sin\frac{\bar{\lambda}A_2}{\delta}|\varsigma|\right]$$

$$N'_{\varsigma\rho} = \frac{\nu(1+m)P}{(1+\nu^2)}$$

$$N'_{\varsigma\varsigma} = \frac{(1+m)P}{(1+\nu^2)} . \qquad (3.3.32)$$

$N'_{\rho\rho}$ is the normal stress resultant directed in the ρ direction. $N'_{\zeta\zeta}$ is a normal stress resultant orthogonal to the ridge (02) . $N'_{\zeta\rho}$ is a shear stress resultant in the plane of the ridge (02) .

The displacement components u_ζ and u_ρ could now be calculated. As in the solution for the valley (12) , it is not possible to make the displacement u_ζ zero everywhere along the ridge. These quantities do not add significantly to the solution and are not presented.

Case II

$$q^2 \equiv \frac{4\gamma^2 k^2}{m^2 \bar{p}^2} - 1 < 0 \tag{3.3.33}$$

Let

$$p^2 \equiv 1 - \frac{4\gamma^2 k^2}{m^2 \bar{p}^2} = -q^2 \tag{3.3.34}$$

then

$$\left.\begin{aligned} y_{21} &= b_{19} e^{\bar{\lambda} A_3 \eta} + b_{20} e^{\bar{\lambda} A_4 \eta} \\ f_{21} &= -\frac{m\bar{p}}{2k}\left(b_{19} A_4^2 e^{\bar{\lambda} A_3 \eta} + b_{20} A_3^2 e^{\bar{\lambda} A_4 \eta} + b_{22}\eta \right) \\ \eta &< 0 \end{aligned}\right\} \tag{3.3.35}$$

$$
\left.
\begin{aligned}
y_{21} &= b_{21} e^{-\lambda A_3 \eta} + b_{22} e^{-\lambda A_4 \eta} \\
f_{21} &= \frac{-m\bar{P}}{2k}\left[b_{21} A_4^2 e^{-\lambda A_3 \eta} + b_{22} A_3^2 e^{-\lambda A_4 \eta} + b_{24}\eta \right] \\
\eta &> 0 .
\end{aligned}
\right\} \qquad (3.3.36)
$$

The use of the symmetry and continuity conditions to evaluate the constants as in Case I gives

$$
\left.
\begin{aligned}
b_{19} = b_{21} &= \frac{-2A_4^2(\alpha_2+\alpha_3-\alpha_4)}{\bar{\lambda} A_3 (A_3^2 - A_4^2)} \\
b_{20} = b_{22} &= \frac{2A_3^2(\alpha_2+\alpha_3-\alpha_4)}{\bar{\lambda} A_4 (A_3^2 - A_4^2)} \\
b_{23} = b_{24} &= 4(\alpha_2+\alpha_3-\alpha_4) .
\end{aligned}
\right\} \qquad (3.3.37)
$$

Thus the functions y' and f' are

$$y' = -\alpha_2 - (\alpha_2+\alpha_3-\alpha_4)(\rho+\xi) + (\alpha_2+\alpha_3-2\alpha_4+4\alpha_5)(\rho-\xi)$$

$$+ (\alpha_4-4\alpha_5)(\rho-\xi)^2 - \frac{2\delta(\alpha_2+\alpha_3-\alpha_4)}{\bar{\lambda}}\left[\frac{A_4^2}{A_3(A_3^2-A_4^2)}e^{\bar{\lambda}A_3\eta}\right.$$

$$\left. - \frac{A_3^2}{A_4(A_3^2-A_4^2)}e^{\bar{\lambda}A_4\eta}\right]$$

$$f' = \frac{(1+m)\bar{P}\ell_5^2}{8\ell^2}(\rho-\xi)^2 + \frac{\delta m\bar{P}(\alpha_2+\alpha_3-\alpha_4)}{\bar{\lambda}k}\left[2\bar{\lambda}\eta + \frac{A_4^4}{A_3(A_3^2-A_4^2)}\right.$$

$$\left. e^{\bar{\lambda}A_3\eta} - \frac{A_3^4}{A_4(A_3^2-A_4^2)}e^{\bar{\lambda}A_4\eta}\right] \qquad (3.3.38)$$

$\xi < 0$

$$y' = -\alpha_2 + (\alpha_2+\alpha_3-\alpha_4)(\rho+\xi) - (\alpha_2+\alpha_3-4\alpha_5)(\rho-\xi)$$

$$+ (\alpha_4-4\alpha_5)(\rho-\xi)^2 - \frac{2\delta(\alpha_2+\alpha_3-\alpha_4)}{\bar{\lambda}}\left[\frac{A_4^2}{A_3(A_3^2-A_4^2)}e^{-\bar{\lambda}A_3\eta}\right.$$

$$\left. - \frac{A_3^2}{A_4(A_3^2-A_4^2)}e^{-\bar{\lambda}A_4\eta}\right] \qquad (3.3.39)$$

$$f' = \frac{(1+m)\bar{P}l_s^2}{8l^2}(e-\varsigma)^2 - \frac{8m\bar{P}(a_2+a_3-a_4)}{\bar{\lambda}k}\left[2\bar{\lambda}\eta - \frac{A_4^4}{A_3(A_3^2-A_4^2)}\right.$$

$$\left. e^{-\bar{\lambda}A_3\eta} + \frac{A_3^4}{A_4(A_3^2-A_4^2)}e^{-\bar{\lambda}A_4\eta}\right] \qquad \left.\right\} (3.3.39)$$

$\varsigma > 0$.

Equations (3.3.38) and (3.3.39), are written in terms of the original variables;

$$w' = -a_2 - 2(a_2+a_3-a_4)(1+\frac{\bar{x}}{l_x}) + 2(a_2+a_3-2a_4+4a_5)\frac{\bar{s}}{l_s}$$

$$+4(a_4-4a_5)\frac{\bar{s}^2}{l_s^2} - \frac{2\delta(a_2+a_3-a_4)}{\bar{\lambda}}\left[\frac{A_4^2}{A_3(A_3^2-A_4^2)}e^{\frac{\bar{\lambda}A_3\varsigma}{\delta}}\right.$$

$$\left. - \frac{A_3^2}{A_4(A_3^2-A_4^2)}e^{\frac{\bar{\lambda}A_4\varsigma}{\delta}}\right] \qquad (3.3.40)$$

$$F' = \frac{(1+m)\bar{P}}{2}\bar{s}^2 + \frac{8mP(a_2+a_3-a_4)l^2}{\bar{\lambda}knh}\left[\frac{2\bar{\lambda}}{\delta}\varsigma + \frac{A_4^4}{A_3(A_3^2-A_4^2)}\right.$$

$$\left. e^{\frac{\bar{\lambda}A_3\varsigma}{\delta}} - \frac{A_3^4}{A_4(A_3^2-A_4^2)}e^{\frac{\bar{\lambda}A_4\varsigma}{\delta}}\right]$$

$\varsigma < 0$

$$w' = -a_2 + 2(a_2+a_3-a_4)(1+\frac{\bar{x}}{\ell_x}) - 2(a_2+a_3-4a_5)\frac{\bar{s}}{\ell_s}$$

$$+ 4(a_4-4a_5)\frac{\bar{s}^2}{\ell_s^2} - \frac{2\delta(a_2+a_3-a_4)}{\bar{\lambda}}\left[\frac{A_4^2}{A_3(A_3^2-A_4^2)}e^{-\frac{\bar{\lambda}A_3}{\delta}\varsigma}\right.$$

$$\left. - \frac{A_3^2}{A_4(A_3^2-A_4^2)}e^{-\frac{\bar{\lambda}A_4}{\delta}\varsigma}\right]$$

$$F' = \frac{(1+m)P}{2}\bar{s}^2 + \frac{\delta m P(a_2+a_3-a_4)\ell^2}{\bar{\lambda}knh}\left[-\frac{2\bar{\lambda}}{\delta}\varsigma\right.$$

$$\left. + \frac{A_4^4}{A_3(A_3^2-A_4^2)}e^{-\frac{\bar{\lambda}A_3}{\delta}\varsigma} - \frac{A_3^4}{A_4(A_3^2-A_4^2)}e^{-\frac{\bar{\lambda}A_4}{\delta}\varsigma}\right] \qquad (3.3.41)$$

$$\varsigma > 0.$$

The additional stress are

$$N'_{\bar{x}\bar{x}} = (1+m)P + \frac{mP(a_2+a_3-a_4)\bar{\lambda}\ell^2}{\delta knh\ell_s^2}\left[\frac{A_3A_4^4}{A_3^2-A_4^2}e^{-\frac{\bar{\lambda}A_3}{\delta}|\varsigma|}\right.$$

$$\left. - \frac{A_4A_3^4}{A_3^2-A_4^2}e^{-\frac{\bar{\lambda}A_4}{\delta}|\varsigma|}\right]$$

$$N'_{\bar{x}\bar{s}} = \frac{1}{\mu}\left[N'_{\bar{x}\bar{x}} - (1+m)P\right] \qquad (3.3.42)$$

$$N'_{\bar{s}\bar{s}} = \frac{1}{\mu^2}\left[N'_{\bar{x}\bar{x}} - (1+m)P\right].$$

3.4. Equilibrium Considerations

The force in the shell consists of that in the boundary layers and that in the field. The axial force in a ridge is

$$T_{RX} = 2\int_{-\infty}^{\frac{\bar{x}}{\ell_x}+\frac{1}{2}} F'_{21,\bar{s}\bar{s}}\, d\bar{s} = -\frac{\pi R(1-k)mP}{nk} \tag{3.4.1}$$

while the circumferential force in a valley is

$$T_V = 2\int_0^{\infty} F_{11,xx}\, dx = \frac{\pi R(1-k)mP}{\mu nk} \tag{3.4.2}$$

The total external load must be equilibrated by the internal force in the shell. Therefore

$$-2\pi RP = 2\pi R(1+m)P - \frac{2n\pi R(1-k)mP}{k} \tag{3.4.3}$$

or

$$m = \frac{k}{1-2k}\,. \tag{3.4.4}$$

A plot of m versus k is shown in Figure 3.3. Note that if m is to be positive then k must be less than one half.

The circumferential and axial equilibrium at a juncture of valleys and ridges is obvious from the symmetry of the deformed shell. The radial equilibrium equation at a joint is satisfied identically by the stresses found and therefore does not give any new information about the shell.

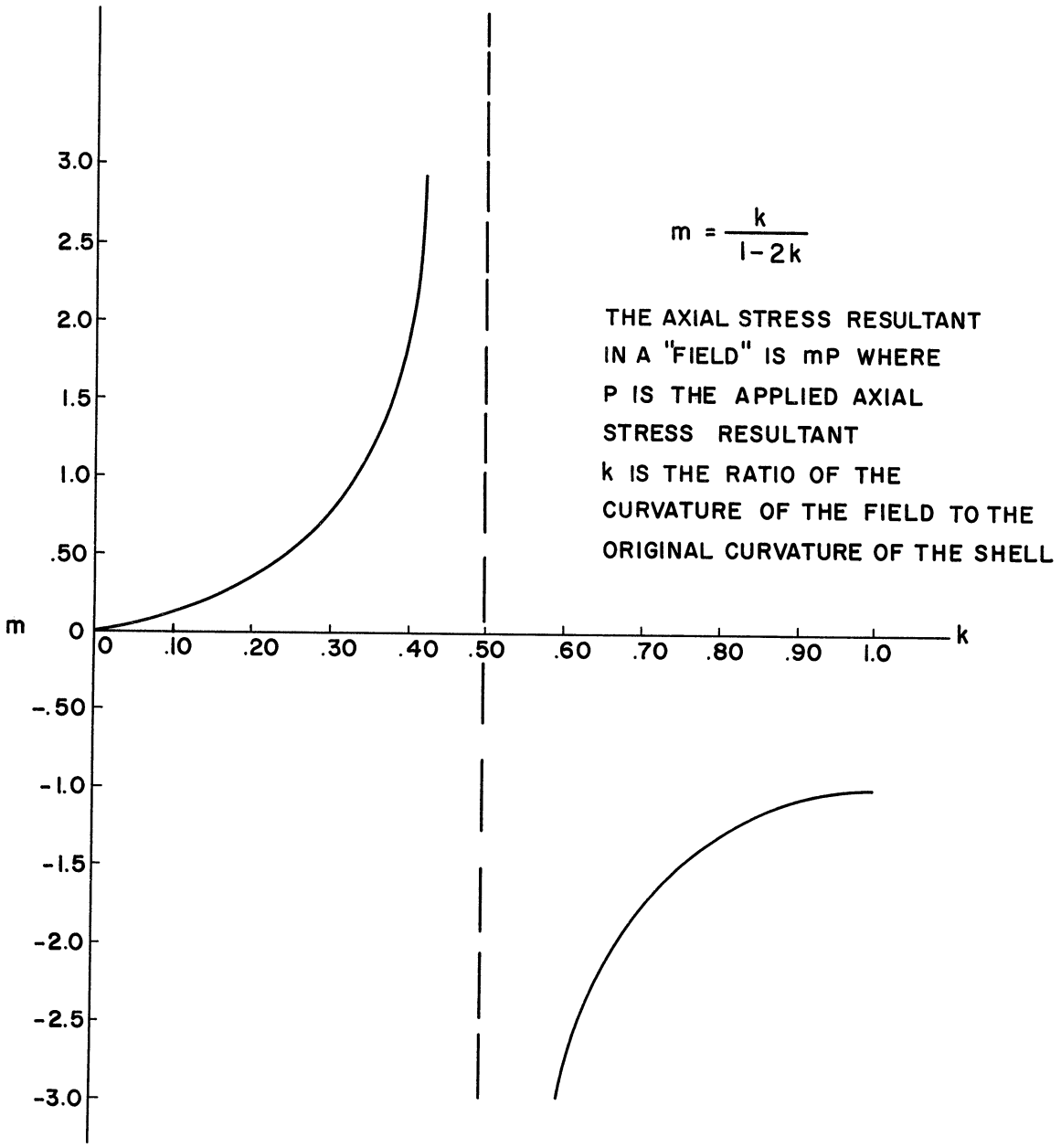

Figure 3.3. Relationship Between m and k for Equilibrium for a Force Prescribed Buckled State.

CHAPTER IV

RESULTS

The results of this work consist of mathematical expressions for the deformations and stresses for a buckled panel of a cylindrical shell. The mathematical expressions and typical graphical representations of them are presented here.

The final buckled shape for the region of the buckled panel which includes a valley is

$$\frac{W+w}{nh} = \frac{\pi^2 k}{2g}(\hat{s}^2-1) - \frac{\pi^2(1-k)}{2g}|\hat{x}| - \frac{\pi^2(1-k)}{8gt} e^{-tA_1|\hat{x}|} \left[\frac{(3A_1^2-A_2^2)}{A_1}\cos tA_2|\hat{x}| - \frac{(3A_2^2-A_1^2)}{A_2}\sin tA_2|\hat{x}|\right] \qquad (q^2>0) \quad (4.1)$$

$$\frac{W+w}{nh} = \frac{\pi^2 k}{2g}(\hat{s}^2-1) - \frac{\pi^2(1-k)}{2g}|\hat{x}| - \frac{\pi^2(1-k)}{2gt}\left[\frac{A_3^2}{A_4(A_3^2-A_4^2)} e^{-tA_4|\hat{x}|} - \frac{A_4^2}{A_3(A_3^2-A_4^2)} e^{-tA_3|\hat{x}|}\right] \qquad (q^2<0) \quad (4.2)$$

in which

$$\left.\begin{aligned} \hat{x} &\equiv \frac{2x}{l_x} & A_1 &\equiv \sqrt{1+\frac{P/P_E}{(1-2k)}} \\ \hat{s} &\equiv \frac{2s}{l_s} & A_2 &\equiv \sqrt{1-\frac{P/P_E}{(1-2k)}} \\ g &\equiv \frac{n^3 h}{R} & A_3 &\equiv \sqrt{\frac{2P/P_E}{(1-2k)}}\sqrt{1-\sqrt{1-\left(\frac{1-2k}{P/P_E}\right)^2}} \end{aligned}\right\} \quad (4.3)$$

$$\nu \equiv \frac{\ell_x}{\ell_s} \qquad A_4 \equiv \sqrt{\frac{2\,P/P_E}{(1-2k)}}\sqrt{1-\sqrt{1-\left(\frac{1-2k}{P/P_E}\right)^2}}$$

$$\tau \equiv \frac{\lambda \ell_x}{2\delta \ell} = \frac{\pi\nu}{2g\gamma}\sqrt{kn} \qquad q^2 \equiv \frac{(1-2k)^2}{(P/P_E)^2} - 1. \qquad (4.3)\ \text{cont'd}$$

The coordinates $\hat{x}$ and $\hat{s}$ are chosen for convenience in displaying the results graphically.

Figure 4.1 shows the buckled shape for an axial section through the panel at $\hat{s} = 0$.

Figure 4.2 shows how the equilibrium configuration changes as a function of the applied axial load.

Figure 4.3 shows how the equilibrium configuration changes as a function of the curvature remaining in the field.

It should be noted that for all of the results shown in Figures 4.1, 4.2 and 4.3, the wavyness of the mathematical solution is not evident because of its relatively long wave length. This is significant since no wavyness has been noted experimentally.

The final buckled shape for a region of the buckled panel which includes a ridge is

$$\frac{W+w'}{nh} = \frac{\pi^2(1-k)}{2g}\left\{(\rho+\varsigma) - \frac{1}{(1-k)}(\rho-\varsigma) + \frac{k}{(1-k)}(\rho-\varsigma)^2 \right.$$

$$+ \frac{(1+\nu^2)}{4\tau} e^{-\frac{2\tau}{(1+\nu^2)}A_1\varsigma}\left[\frac{(3A_1^2-A_2^2)}{A_1}\cos\frac{2\tau}{(1+\nu^2)}A_2\varsigma \right. \qquad (4.4)$$

$$\left.\left. - \frac{(3A_2^2-A_1^2)}{A_2}\sin\frac{2\tau}{(1+\nu^2)}A_2\varsigma\right]\right\} \qquad (\varsigma > 0)$$

$$\frac{W+w'}{nh} = \frac{\pi^2(1-k)}{2g}\left\{-(\rho+\varsigma) + \frac{(1-2k)}{(1-k)}(\rho-\varsigma) + \frac{k}{(1-k)}(\rho-\varsigma)^2\right.$$

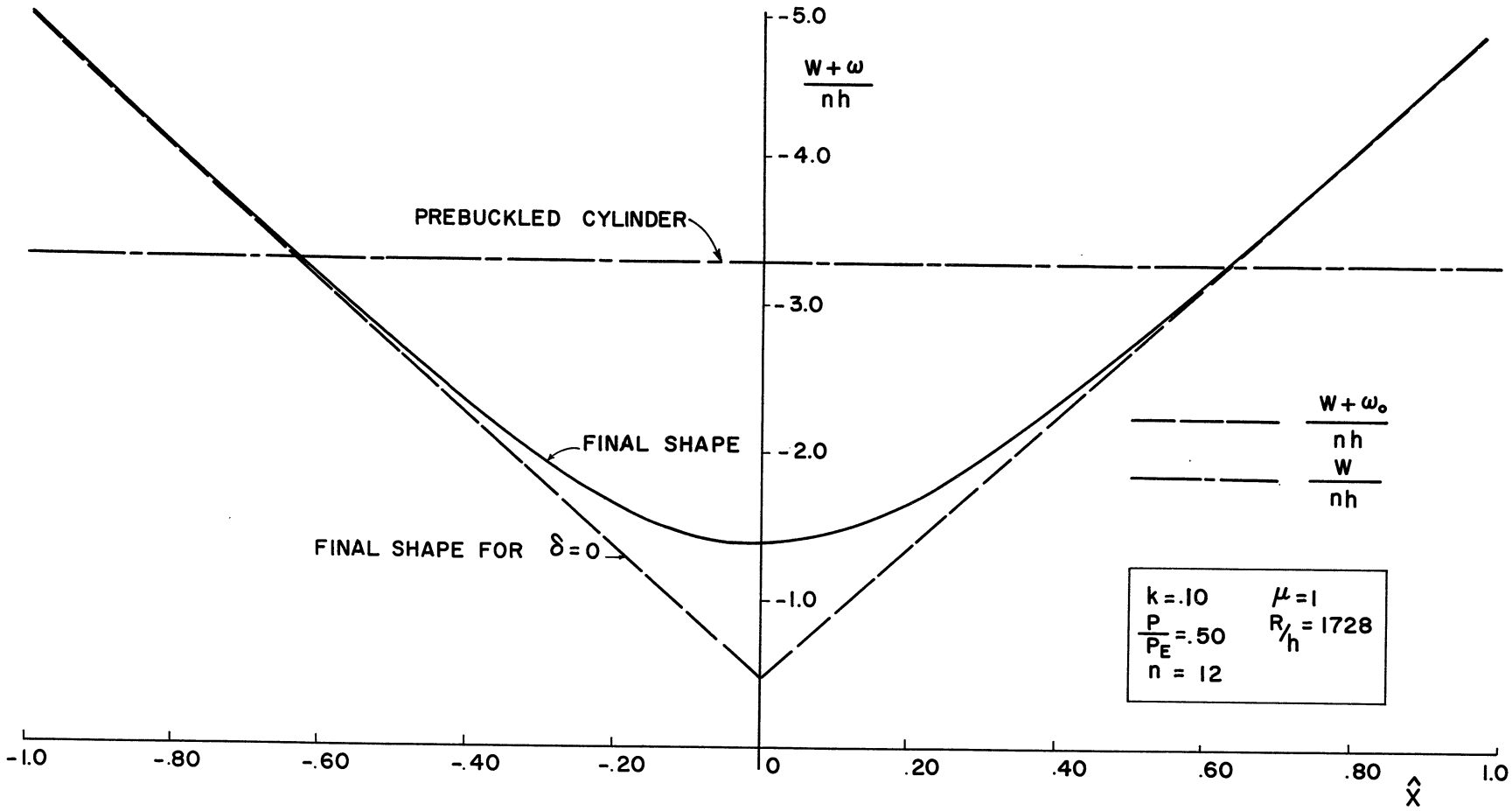

Figure 4.1. Final Shape of the Buckled Panel for $\hat{s} = 0$.

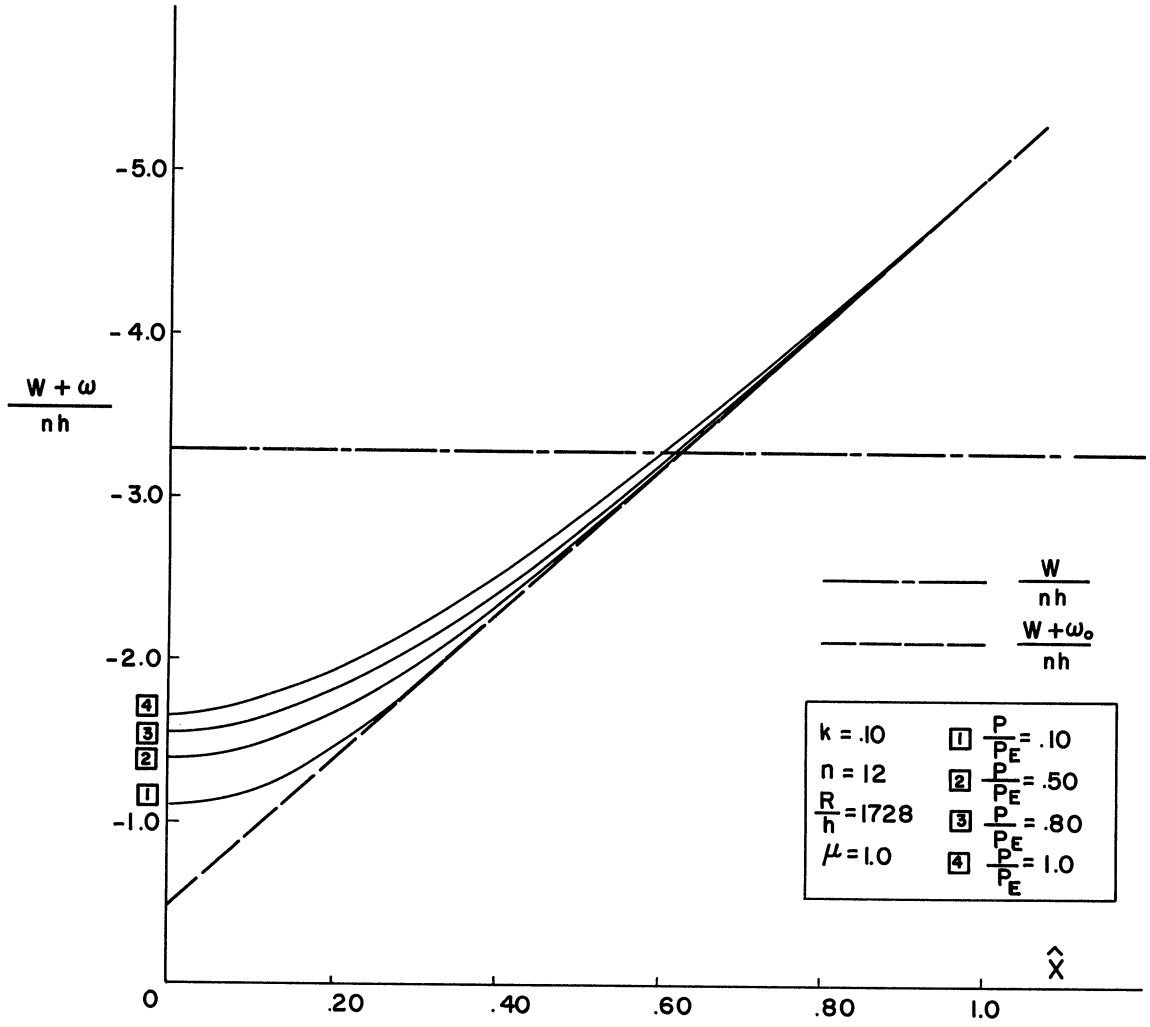

Figure 4.2. Final Shape of the Buckled Panel for $\hat{s} = 0$, $\hat{x} > 0$.

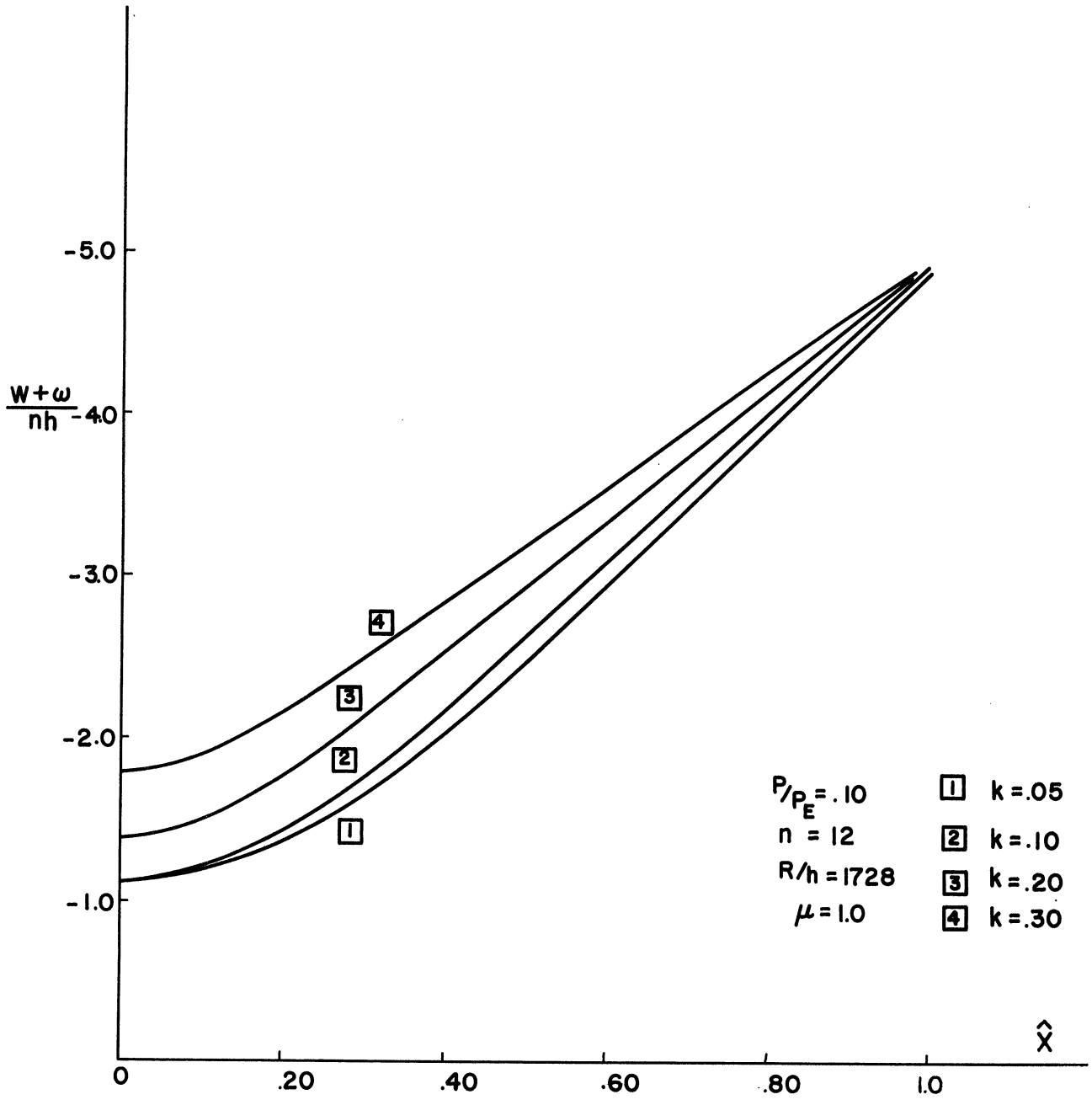

Figure 4.3. Final Shape of the Buckled Panel for $\hat{s} = 0$, $\hat{x} > 0$.

$$+\frac{(1+\nu^2)}{4\tau}e^{\left(\frac{2\tau}{(1+\nu^2)}A_1\varsigma\right)}\left[\frac{(3A_1^2-A_2^2)}{A_1}\cos\frac{2\tau}{(1+\nu^2)}A_2\varsigma\right.$$

$$\left.+\frac{(3A_2^2-A_1^2)}{A_2}\sin\frac{2\tau}{(1+\nu^2)}A_2\varsigma\right] \qquad (\varsigma<0) \qquad (4.5)$$

in which

$$\varrho \equiv \frac{\bar{x}}{\ell_x}+\frac{\bar{s}}{\ell_s}+\frac{1}{2} \qquad \varsigma \equiv \frac{\bar{x}}{\ell_x}-\frac{\bar{s}}{\ell_s}+\frac{1}{2}. \qquad (4.6)$$

Figure 4.4 shows the final buckled shape for a section at $\rho = 0$.

The circumferential stress in a valley is given by the expressions

$$\frac{N_{ss}}{P_E}=\frac{\tau(1-k)P}{4\nu^2(1-2k)P_E}e^{-\tau A_1|\hat{x}|}\left[\left(\frac{1}{A_1}+\frac{q_0}{A_2}\right)\cos\tau A_2|\hat{x}|\right.$$

$$\left.+\left(\frac{1}{A_2}-\frac{q_0}{A_1}\right)\sin\tau A_2|\hat{x}|\right] \qquad (q_0^2>0) \qquad (4.7)$$

$$\frac{N_{ss}}{P_E}=\frac{\tau(1-k)P}{4\nu^2(1-2k)P_E}\left[\frac{A_4A_3^4}{A_3^2-A_4^2}e^{-\tau A_4|\hat{x}|}-\frac{A_3A_4^4}{A_3^2-A_4^2}e^{-\tau A_3|\hat{x}|}\right]. \qquad (4.8)$$
$$(q_0^2<0)$$

Similarly the total stress resultant directed along the ridge is

$$\left(\frac{N'_{\varrho\varrho}+N^{\circ}_{\varrho\varrho}}{P_E}\right)=\frac{\nu^2kP}{(1+\nu^2)(1-2k)P_E}-\frac{\tau(1-k)P}{4\nu(1-2k)P_E}e^{\frac{-2\tau A_1}{(1+\nu^2)}|\varsigma|}$$

$$\left[\left(\frac{1}{A_1}+\frac{q_0}{A_2}\right)\cos\frac{2A_2}{(1+\nu^2)}|\varsigma|+\left(\frac{1}{A_2}-\frac{q_0}{A_1}\right)\sin\frac{2A_2}{(1+\nu^2)}|\varsigma|\right]. \qquad (4.9)$$

Figures 4.5 and 4.6 show how $\frac{N_{ss}}{P_E}$ varies with $\hat{x}$ and how the load parameter P/P_E affects this stress distribution.

Figure 4.7 shows how $\frac{N'_{\rho\rho}}{P_E}$ varies with ζ.

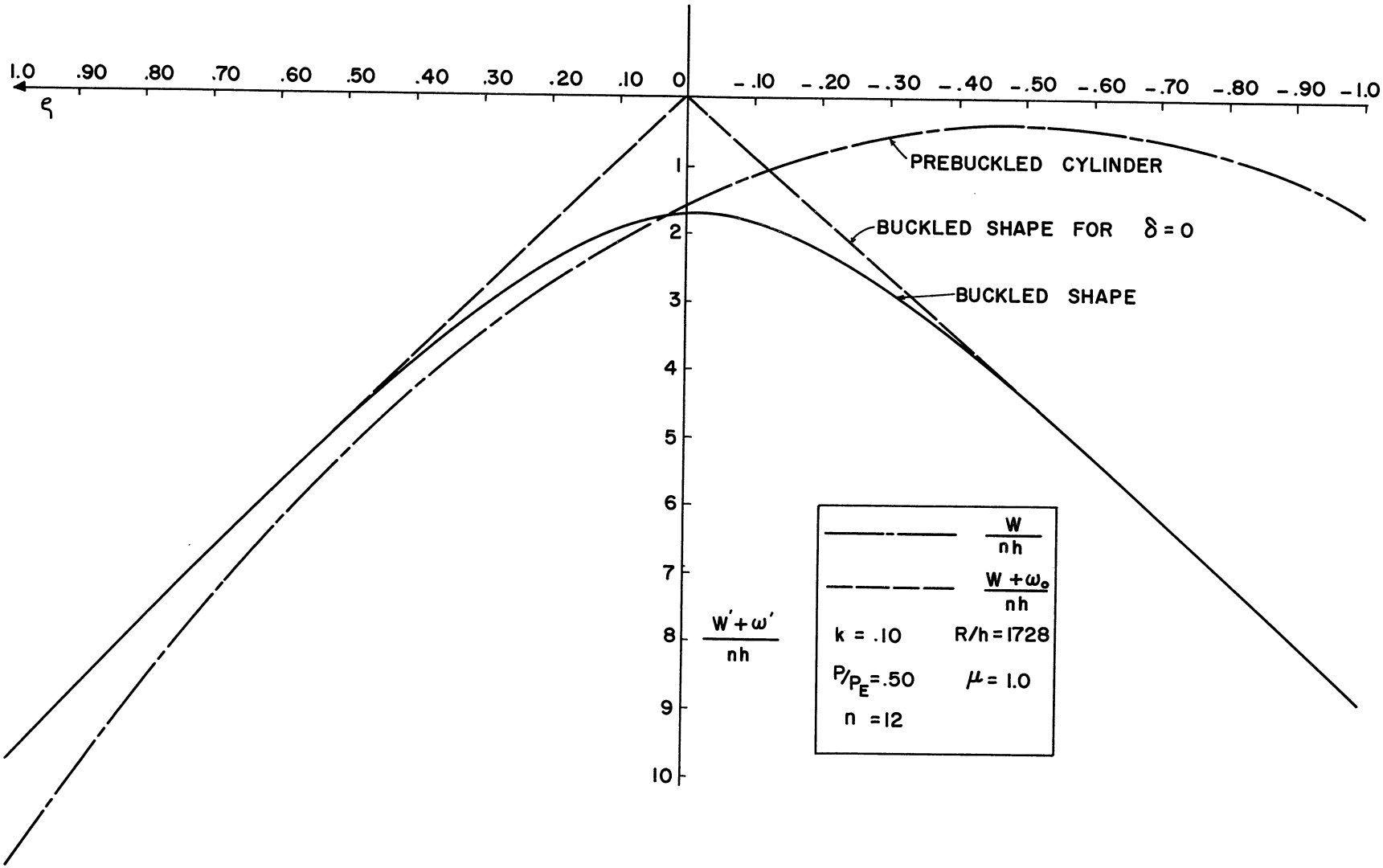

Figure 4.4. Buckled Shape for a Ridge of the Buckled Shell for $\rho = 0$.

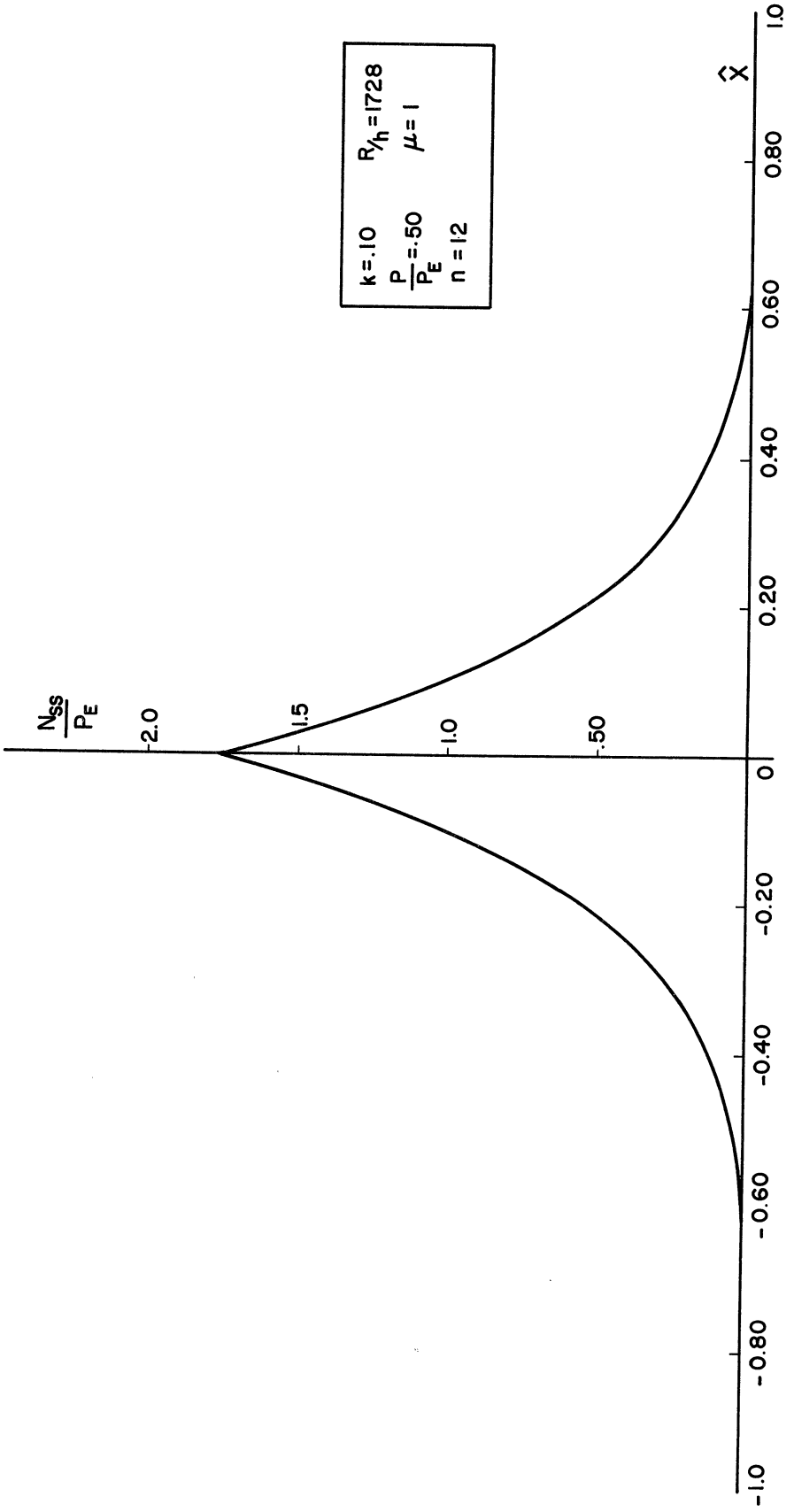

Figure 4.5. Circumferential Stress in a Valley.

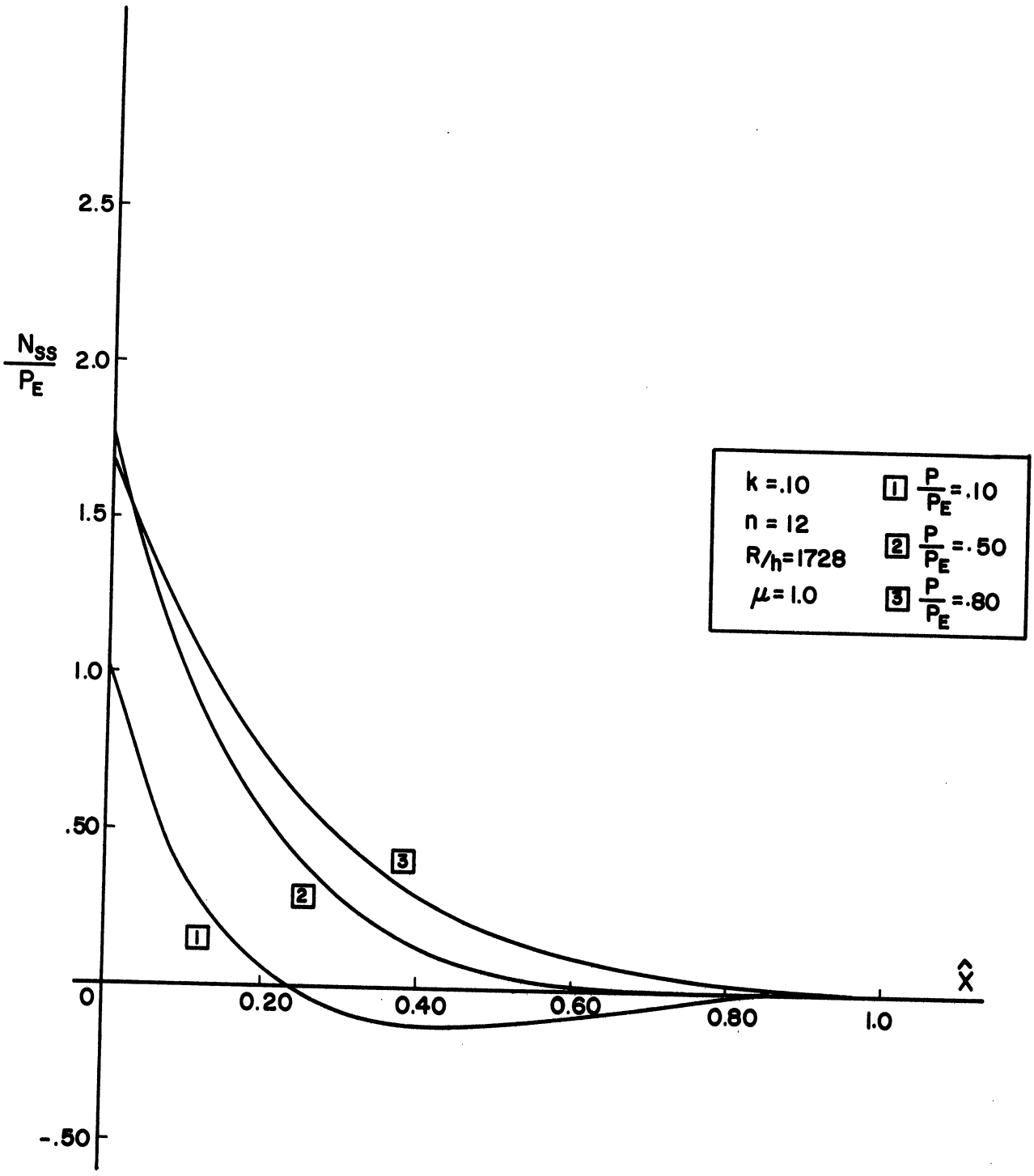

Figure 4.6. Circumferential Stress in a Valley for $x > 0$.

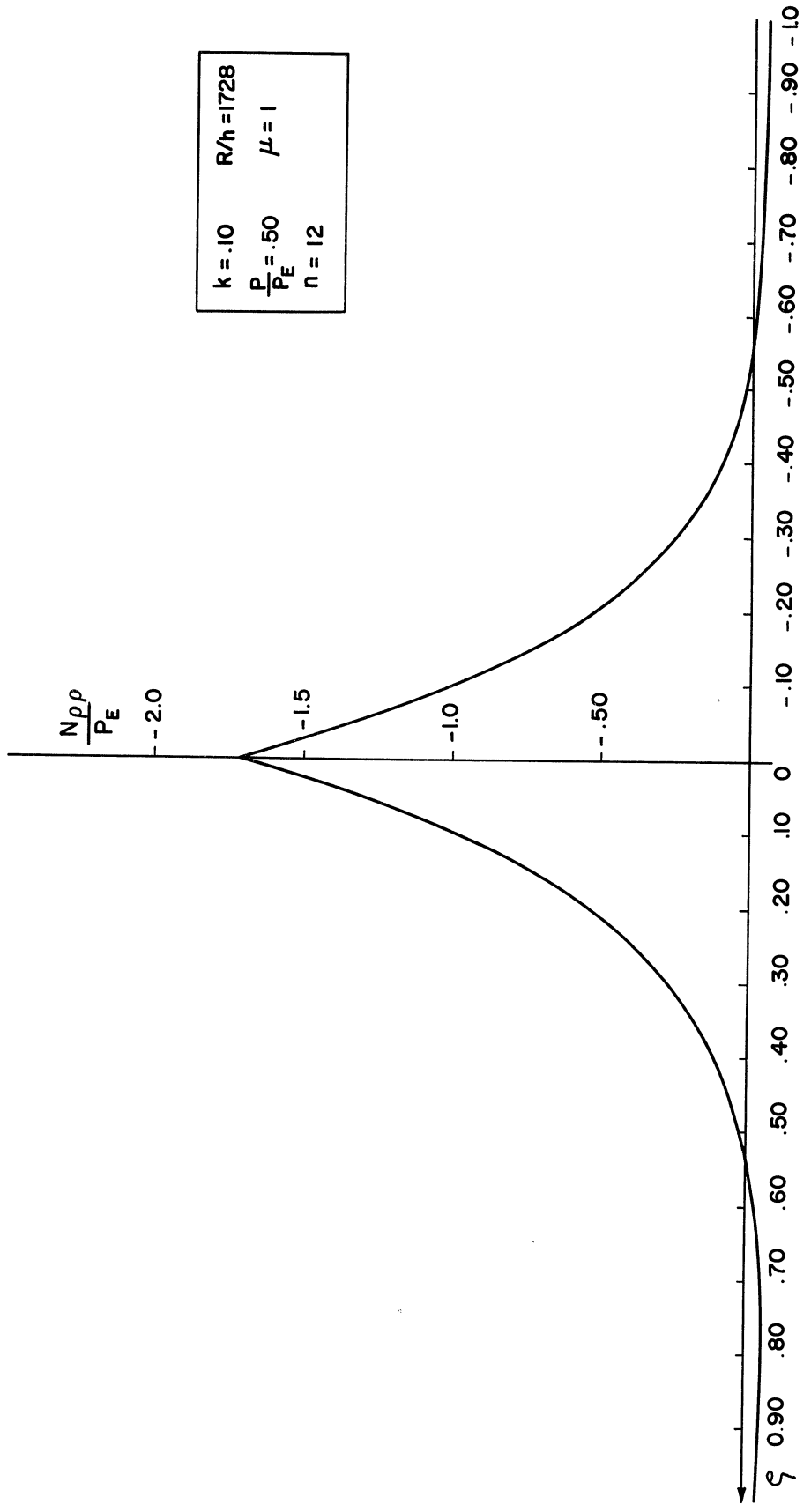

Figure 4.7. Normal Stress Along a Ridge.

The axial tensile stress in the field is given by the expression

$$\left(\frac{N_{xx}-P}{P_E}\right) = \frac{k}{(1-2k)}\frac{P}{P_E} . \qquad (4.10)$$

The significant result here is that if k is significantly less than 1/2, the tensile stress in the field will be small (e.g., for $k = .10$, $\frac{P}{P_E} = .50$, the tensile stress in the field is only $.0625\ P_E$).

The axial displacement u_x can not be made continuous along the valley and the displacement normal to the ridge can not be made continuous at the ridge using the approximations employed herein. A plot of u_x/h along a valley indicates the extent to which the continuity condition at the valley is violated, (Figure 4.8). The magnitude of this discrepancy decreases as k decreases.

The mathematical expressions other than those listed above which were found in this investigation are as follows:

For the region including a valley,

$$\frac{u_x}{h} = \frac{2\pi\gamma(1-k)P}{n(1-2k)P_E} - \frac{\nu\pi\gamma(1-k)P}{\nu n(1-2k)P_E}\left[1 - e^{+A_1\hat{x}}\left(\cos +A_2\hat{x} - \left(\frac{q_0}{2} - \frac{1}{2q_0}\right)\sin +A_2\hat{x}\right)\right] - \frac{\pi^3(1-k)^2}{8\nu g}\left\{\hat{x} + \frac{1}{2+}e^{+A_1\hat{x}}\left[\frac{(3A_1^2-A_2^2)}{A_1}\cos +A_2\hat{x} - \frac{(3A_2^2-A_1^2)}{A_2}\sin +A_2\hat{x}\right] + \frac{1}{8+}e^{-2+A_1\hat{x}}\left[\left(A_2 - \frac{2A_1}{q_0} - \frac{A_2}{q_0^2}\right)\sin +A_2\hat{x} - \left(A_1 + \frac{2A_2}{q_0} - \frac{A_1}{q_0^2}\right)\cos +A_2\hat{x} - \frac{2}{A_1}\left(1+\frac{1}{q_0^2}\right)\right] - \frac{1}{2+}\left[\frac{(3A_1^2-A_2^2)}{A_1} - \frac{1}{4}\left(A_1 + \frac{2A_2}{q_0} - \frac{A_1}{q_0^2}\right) - \frac{1}{2A_1}\left(1+\frac{1}{q_0^2}\right)\right]\right\} + \frac{\pi^3 k(1-k)}{4\nu g}\left(\hat{s}^2 - \frac{1}{3}\right) \qquad (u_x>0)(q_0^2>0) \qquad (4.11)$$

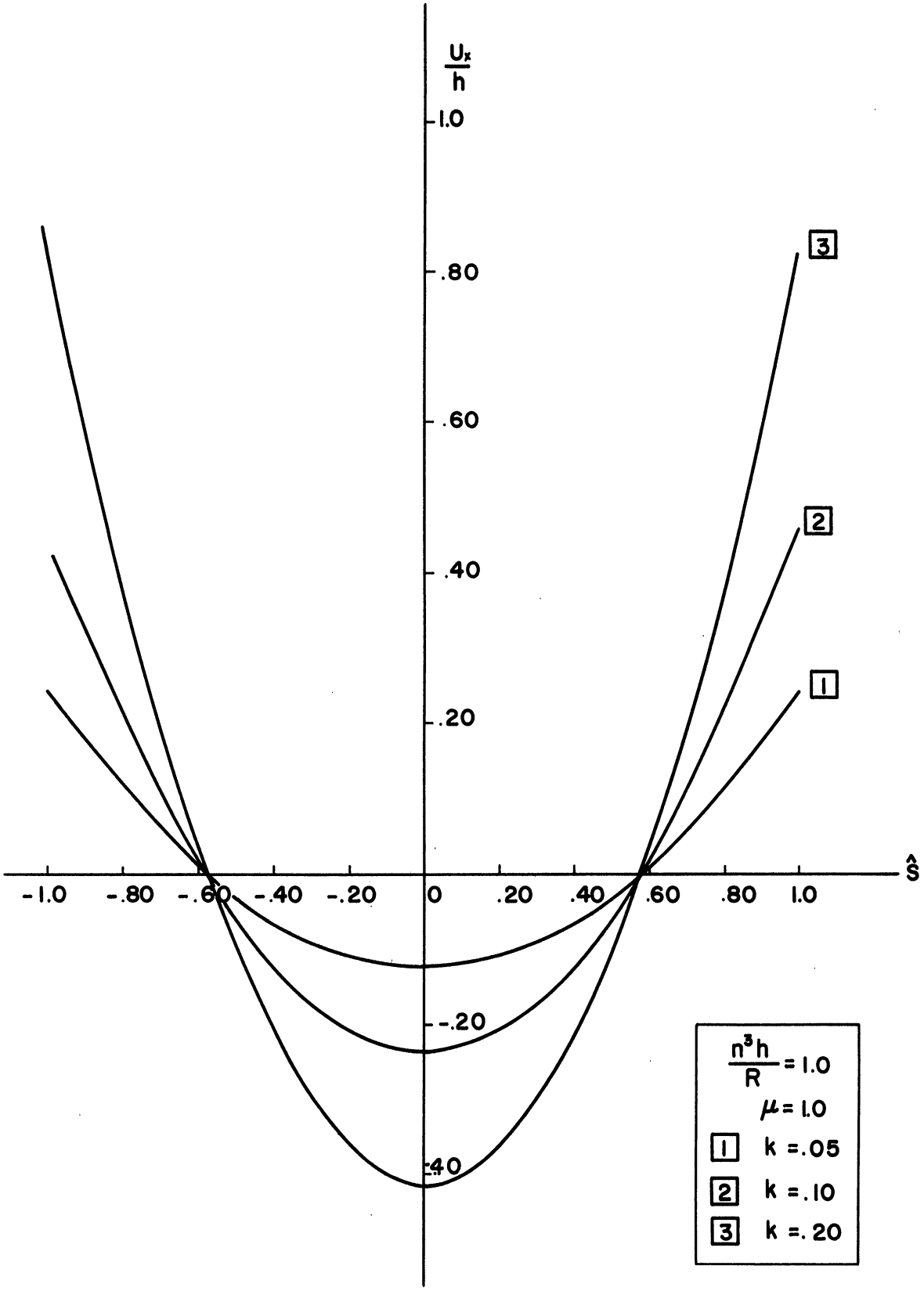

Figure 4.8. Axial Displacement $\frac{u_x}{h}$ Along the Line $\hat{x} = 0$.

$$\frac{u_x}{h}(\hat{x}<0) = -\frac{u_x}{h}(\hat{x}>0) \tag{4.12}$$

$$\frac{u_s}{h} = \frac{2\pi\nu\gamma(1-k)P}{n(1-2k)P_E}\hat{s} + \frac{\pi\gamma+(1-k)P}{2\nu^2 n(1-2k)P_E} e^{-+A_1|\hat{x}|}\left[\left(\frac{1}{A_1}+\frac{q}{A_2}\right)\right.$$

$$\cos+A_2|\hat{x}| + \left(\frac{1}{A_2}-\frac{q}{A_1}\right)\sin+A_2|\hat{x}|\Big]\hat{s} +$$

$$\frac{\pi^3(1-k^2)}{6g}\hat{s}^3 \qquad (q^2>0)$$

$$\frac{u_x}{h} = \frac{2\pi\nu\gamma(1-k)P}{n(1-2k)P_E}\hat{x} - \frac{\pi\nu\gamma(1-k)P}{2\nu n(1-2k)P_E}\left[2-\frac{A_3^4}{A_3^2-A_4^2}e^{-+A_4\hat{x}}\right.$$

$$+\frac{A_4^4}{A_3^2-A_4^2}e^{-+A_3\hat{x}}\Big] - \frac{\pi^3(1-k)^2}{8\nu g}\left\{\hat{x}+\frac{2A_4^2}{+A_3(A_3^2-A_4^2)}\left(1-\right.\right.$$

$$e^{-+A_3\hat{x}}\Big) - \frac{2A_3^2}{+A_4(A_3^2-A_4^2)}\left(1-e^{-+A_4\hat{x}}\right) - \frac{2A_3^2A_4^2}{+(A_3+A_4)(A_3^2-A_4^2)^2}$$

$$\left(1-e^{-+(A_3+A_4)\hat{x}}\right) + \frac{A_4^4}{2+(A_3^2-A_4^2)^2A_3}\left(1-e^{-2+A_3\hat{x}}\right)$$

$$\left.+\frac{A_3^4}{2+A_4(A_3^2-A_4^2)^2}\left(1-e^{-2+A_4\hat{x}}\right)\right\} + \frac{\pi^3k(1-k)}{4\nu g}\left(\hat{s}^2-\frac{1}{3}\right) \qquad (q^2<0)$$

$$\frac{u_s}{h} = -\frac{2\pi\nu\gamma(1-k)P}{n(1-2k)P_E}\hat{s} + \frac{\pi\gamma+(1-k)P}{2\nu^2 n(1-2k)P_E}\left[\frac{A_4A_3^4}{A_3^2-A_4^2}e^{-+A_4|\hat{x}|}\right.$$

$$\left.-\frac{A_3A_4^4}{A_3^2-A_4^2}e^{-+A_3|\hat{x}|}\right]\hat{s} + \frac{\pi^3(1-k^2)}{6g}\hat{s}^3 \qquad (q^2<0)$$

$$N_{xs} = 0 . \tag{4.16}$$

For a region including a ridge,

$$\frac{N'_{ep}}{P_E} = \frac{(1-k)\,P}{(1+\nu^2)(1-2k)\,P_E} \tag{4.17}$$

$$\frac{N'_{sp}}{P_E} = \frac{\nu(1-k)P}{(1+\nu^2)(1-2k)\,P_E} . \tag{4.18}$$

CHAPTER V

CONCLUSIONS

The solution, presented in this work, to the problem of finding an equilibrium configuration for a buckled cylindrical shell is not exact, since the axial displacement can not be made continuous within the approximations used in the analysis (Figure 4.8). The effects of the interactions between the ridges and valleys of the buckled shape were also not considered. However, the nature of the results seems to indicate that this is a reasonable approximation to the theoretical determination of the postbuckled state of the shell.

The solution was carried out by assuming some residual curvature in the field of the buckled state. There is little experimental evidence to indicate that the buckles are not flat. The results however indicate that very little curvature is necessary in the buckled state; the experimental evidence is therefore inconclusive (Figure 4.1). The amount of the discontinuity in the axial displacement decreases as the buckle becomes flatter (Figure 4.8).

Comparing the experimental buckled shape with the theoretical shape is further complicated by the fact that when buckling has progressed to the point where the valleys and ridges are sharply defined, the shell material will have yielded and the effects of having a nonelastic material will become apparent.

An improvement in the solution could conceivably be obtained by considering higher order terms in the expansions of the boundary layer functions. Another possibility would be to consider the field stress to be nonuniform. The curvature necessary for the boundary layer might also be considered to be inherent in the boundary layer rather than the field. These observations are speculation and no proof that they will work is available.

One interesting result of this investigation is the fact that the no unique equilibrium load was found, since many buckled configurations are possible for the same external load (i.e., Many values of k are possible (Figure 4.3)).

This work sheds no light on the problem of how the shell departs from the prebuckled state. However, it has shown that a buckled equilibrium configuration which resembles quite well the buckled shell can be found analytically and that the axial load necessary for equilibrium is significantly less than the buckling load. This agrees with the experimental work on this problem.

APPENDIX A

GEOMETRIC RELATIONS FOR THE BUCKLED SHELL

The relations between the shell deformation parameters a_2, a_3, a_4, a_5, n and k and the natural shell parameters R and h are developed in this appendix.

The deformation in the field is assumed to be inextensiable, therefore

$$\chi = k \frac{\pi}{n} . \tag{A-1}$$

It follows from the geometry of the deformation that

$$a_1 \cos \frac{\pi}{n} = a_2 . \tag{A-2}$$

For large n $\frac{\pi^2}{2n^2}$ is negligible when compared with 1, therefore

$$a_1 \approx a_2 . \tag{A-3}$$

Other geometric relationships are

$$a_2 + a_3 = R(1 - \cos \frac{\pi}{n}) \tag{A-4}$$

$$R/k \sin\chi = (R + a_1) \sin \frac{\pi}{n} \tag{A-5}$$

$$a_4 = R/k \, (1 - \cos\chi) . \tag{A-6}$$

a_2 is found by substituting (A-2) in (A-5) to give

$$a_2 = \frac{R}{k} \sin k \frac{\pi}{n} \cot \frac{\pi}{n} - R \cos \frac{\pi}{n} . \tag{A-7}$$

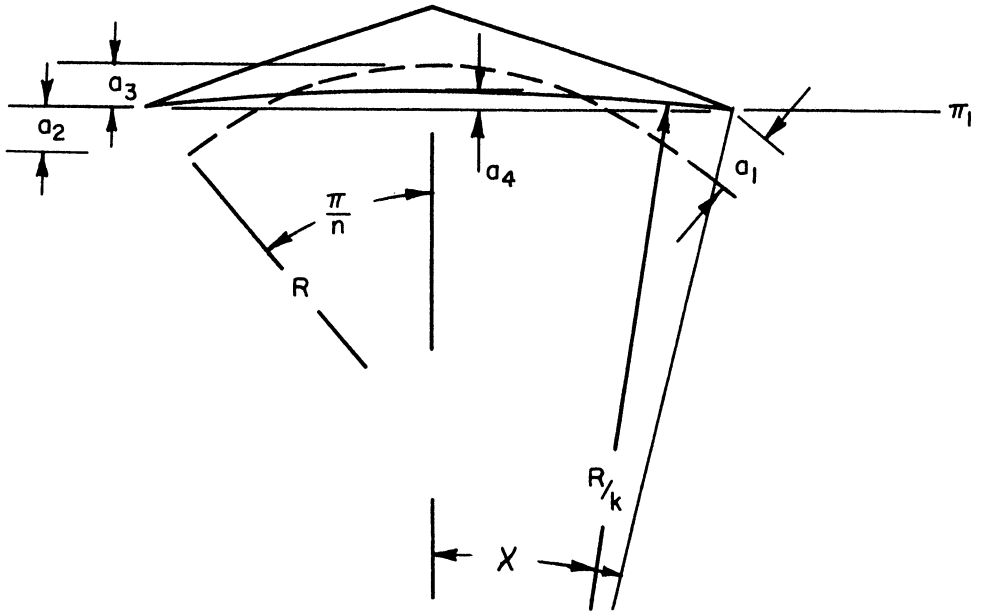

Figure A-1. Geometry of a Buckled Panel.

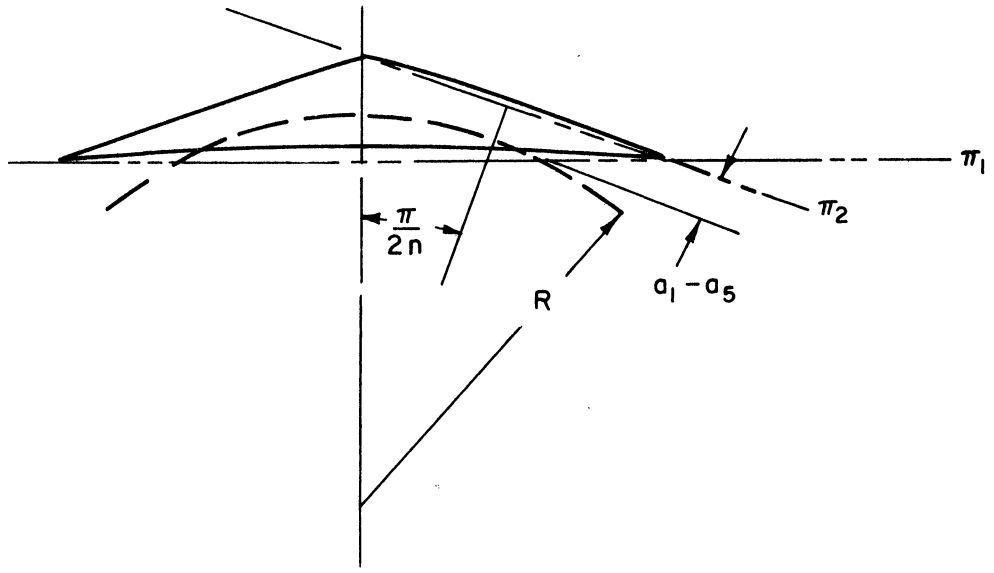

Figure A-2. Geometry of a Buckled Panel.

a_3 is now calculated using (A-7) and (A-4), this gives

$$a_3 = R\left(1 - \frac{1}{k} \sin k\frac{\pi}{n} \cot\frac{\pi}{n}\right). \qquad \text{(A-8)}$$

Again as in Equation (A-3) the assumption of $\frac{\pi}{n}$ a small angle leads to

$$a_2 \fallingdotseq \frac{\pi^2 R}{6n^2}(1 - k^2) \qquad \text{(A-9)}$$

$$a_3 \fallingdotseq \frac{\pi^2 R}{6n^2}(2 - k^2) \qquad \text{(A-10)}$$

$$a_4 \fallingdotseq \frac{\pi^2 R}{2n^2} k \qquad \text{(A-11)}$$

It follows from the geometry of the shell that

$$(R + a_1)\cos\frac{\pi}{2n} = R + a_1 - a_5. \qquad \text{(A-12)}$$

In line with the approximations being employed a_5 is found to be

$$a_5 \approx \frac{\pi^2 R}{8n^2}, \qquad \text{(A-13)}$$

The following combinations appear in the text:

$$a_3 - a_4 \approx \frac{\pi^2 R}{6n^2}(1 - k)(2 - k) = \frac{\pi^2 nh}{6g}(1 - k)(2 - k) \qquad \text{(A-14)}$$

$$a_2 + a_3 - a_4 \approx \frac{\pi^2 R}{2n^2}(1 - k) = \frac{\pi^2 nh}{2g}(1 - k) \qquad \text{(A-15)}$$

$$\frac{a_2 + a_3 - a_4}{\ell_x} \fallingdotseq \frac{\pi}{4\mu n}(1 - k) \qquad \text{(A-16)}$$

$$a_4 - 4a_5 \backsimeq \frac{\pi^2 R}{2n^2}(1 - k) = \frac{\pi^2 nh}{2g}(1 - k) \qquad \text{(A-17)}$$

$$a_2 + a_3 - 2a_4 + 4a_5 \backsimeq \frac{\pi^2 R}{n^2}(1 - k) = \frac{\pi^2 nh}{g}(1 - k) \qquad \text{(A-18)}$$

$$a_2 + a_3 - 4a_5 \backsimeq 0 . \qquad \text{(A-19)}$$

Another useful relationship which has been used in the text is

$$\frac{\bar{m}}{k} = \frac{m\ell_s^2}{8\ell^2\alpha_4} = \frac{m}{8}\left(\frac{4\pi^2R^2}{n^2}\right)\left(\frac{1}{nRh}\right)\left(\frac{2n^3h}{\pi^2Rk}\right) = \frac{m}{k} . \qquad \text{(A-20)}$$

APPENDIX B

EQUILIBRIUM CONSIDERATIONS

If the limiting case of an extremely thin shell is considered so that in the buckled shape the ridges and valleys are lines, it can be shown that the field must have a tensile stress.

Consider the equilibrium of a valley in the z direction. Let T_v, the force in the valley, be tensile, then if the final shape of the valley has some curvature, as has been assumed, a component of this force in the positive z direction will exist.

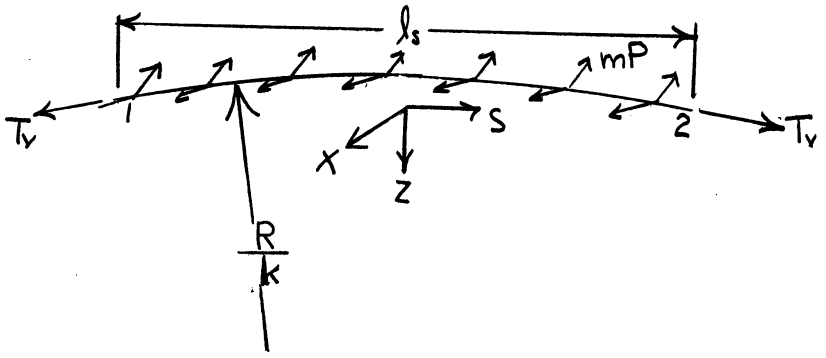

Figure B-1. Equilibrium of a Valley.

The z component of the force in a valley is

$$T_{vz} = T_v \left.\frac{\partial(w_o+W)}{\partial S}\right|_{S=\pm\frac{l_s}{2},\,X=0} \tag{B-1}$$

or

$$T_{vz} = \frac{T_v k l_s}{2R} . \tag{B-2}$$

The only way that this valley could be in equilibrium is for an axial tensile stress to exist in the field. If this stress is assumed to be uniform, then the z component of the force in the field is

$$T_{FZ} = mP\ell_s \frac{\partial(W+W_0)}{\partial X} \tag{B-3}$$

or

$$T_{FZ} = \frac{2mP}{\rho}(a_2 + a_3 - a_4). \tag{B-4}$$

An equilibrium requirement is that the resulting force in the z direction equal to zero. That is,

$$2T_{FZ} - 2T_{VZ} = 0 . \tag{B-4}$$

If follows from (B-2), (B-4) and (B-5) that

$$T_V = \frac{\pi R(1 - k)mP}{\mu nk} . \tag{B-6}$$

If the force T_V is compressive then the field stress is also compressive.

In contrast if the equilibrium of a ridge is considered in the same way the conclusion is that for a tensile axial stress in the field the force in the ridge is compressive.

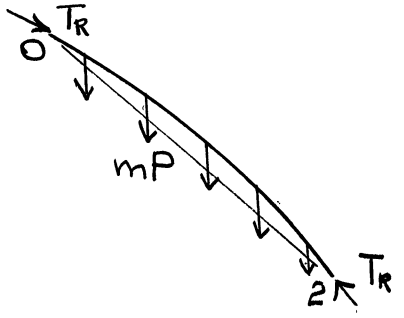

Figure B-2. Equilibrium of a Ridge.

The z component of the force in a ridge is

$$T_{Rz} = T_R \frac{\partial(W+W_o')}{\partial \rho} \frac{2}{l_s\sqrt{1+\mu^2}} = T_R \frac{2a_4}{l_s\sqrt{1+\mu^2}} \tag{B-7}$$

The z component of the force in the field is

$$T_{FZ} = mP \frac{\partial(W+W_o')}{\partial \bar{x}} \frac{l_s}{2} = \frac{mP(a_2+a_3-a_4)}{\mu} \tag{B-8}$$

Again since there are two ends and two sides to the ridge

$$\frac{2mP(a_2+a_3-a_4)}{\mu} = \frac{2T_R a_4}{l_s\sqrt{1+\mu^2}} \tag{B-9}$$

or

$$T_R = \frac{\pi R\sqrt{1+\mu^2}(1-k)mP}{\mu k n} \tag{B-10}$$

It should be noted that the Equation (B-6) agrees with Equation (3.4.2) and if the x component of (B-10) were to be found it would be the same as (3.4.1).

Since a compressive external load is being considered the forces in the ridges should be compressive; this leads to the conclusion that a tensile field stress must exist.

It is important to note, at this point, that the conclusion that a tensile stress in the field must exist can also be drawn on less physical grounds. A negative value of m does not allow for a buckled shape which closely resembles the observed shape since solutions to the boundary layer equations for negative m to not decay as the coordinate normal to the boundary increases.

APPENDIX C

EXPERIMENTAL RESULTS

To demonstrate the validity of the assumption that in the buckled state $\frac{n^3h}{R}$ is near one in value, typical experimental results are quoted. For comparison $\frac{n^2h}{R}$ is also calculated.

Investigator	n	R/h	$\frac{n^3h}{R}$	$\frac{n^2h}{R}$
Tennyson (31)	6	154	1.40	.23
Lundquist (7)	9-10	333-362	2.01-3.33	.224-.33
	10	455-460	2.2	.22
	10-13	625-714	1.4-3.5	.14-.27
	11	679-757	1.7-2.0	.16-.18
	11-13	909-920	1.4-2.4	.13-.19
	12-15	1270-1415	1.2-2.7	.10-.18
Donnell (17)	10	483	2.1	.21
	12	1284	1.3	.11
	10.5	1383	.84	.08
	8	314	1.6	.20
	10	897	1.1	.11

APPENDIX D

SOLUTION OF THE BOUNDARY LAYER EQUATIONS

The solution of Equation (3.2.15) is presented in this Appendix. Equation (3.2.15) is

$$\left.\begin{aligned} \gamma^2 \frac{d^4 Y_{11}}{d\psi^4} - m\bar{P}\frac{d^2 Y_{11}}{d\psi^2} - k\frac{d^2 f_{11}}{d\psi^2} &= 0 \\ \frac{d^4 f_{11}}{d\psi^4} + k\frac{d^2 Y_{11}}{d\psi^2} &= 0. \end{aligned}\right\} \qquad \text{(D-1)}$$

Let

$$\left.\begin{aligned} Y_{11} &= c_i e^{\hat{\lambda}_i \psi} \\ f_{11} &= d_i e^{\hat{\lambda}_i \psi} \end{aligned}\right\} \qquad i = 1, 2, 3, \ldots 8 \qquad \text{(D-2)}$$

The substitution of (D-2) in (D-1) leads to

$$c_i(\gamma^2 \hat{\lambda}_i^4 - m\bar{P}\hat{\lambda}_i^2) - d_i k \hat{\lambda}_i^2 = 0 \qquad \text{(D-3)}$$

$$c_i k \hat{\lambda}_i^2 + d_i \hat{\lambda}_i^4 = 0. \qquad \text{(D-4)}$$

For a nontrivial solution to (D-3) and (D-4) to exist

$$\hat{\lambda}_i^4 (\hat{\lambda}_i^4 - m\bar{P}\hat{\lambda}_i^2 + k^2) = 0. \qquad \text{(D-5)}$$

The roots $\hat{\lambda}_i = 0$ are not associated with exponentially decaying solutions but with polynomial solutions. These polynomial

solutions must be rejected for y_{11} since all solutions must decay as $|\psi|$ increases. A polynomial of first order will not effect the stresses and can be retained. Such a solution will be necessary to satisfy the condition that f,ξ be zero at $\xi = 0$.

The four roots to (D-5) which give rise to exponential solutions are

$$\hat{\lambda}_i = \pm\sqrt{\frac{m\bar{p}}{2\gamma^2}\left[1 \pm \sqrt{1 - \frac{4\gamma^2 k^2}{m^2\bar{p}^2}}\right]} \qquad i = 1, 2, 3, 4 \qquad \text{(D-6)}$$

Case I

$$\frac{4\gamma^2 k^2}{m^2\bar{p}^2} > 1 \qquad \text{(D-7)}$$

Let

$$q^2 \equiv \frac{4\gamma^2 k^2}{m^2\bar{p}^2} - 1 \quad . \qquad q^2 > 0 \qquad \text{(D-8)}$$

Then

$$\hat{\lambda}_i = \pm\sqrt{\frac{m\bar{p}}{2\gamma^2}}\sqrt{1 \pm iq} \quad . \qquad \text{(D-9)}$$

To facilitate the solution the following parameters are defined:

$$\left.\begin{aligned} \sin\theta &\equiv \frac{q}{\sqrt{1+q^2}} \\ \cos\theta &\equiv \frac{1}{\sqrt{1+q^2}} \\ \lambda &\equiv \sqrt{k/2\gamma} \\ A_1 &\equiv \sqrt{2\cos\frac{\theta}{2}} \\ A_2 &\equiv \sqrt{2\sin\frac{\theta}{2}} \quad . \end{aligned}\right\} \qquad \text{(D-10)}$$

The use of (D-10) allows the roots (D-9) to be expressed as

$$\begin{aligned}
\hat{\lambda}_1 &= \lambda(A_1 + iA_2) \\
\hat{\lambda}_2 &= -\lambda(A_1 + iA_2) \\
\hat{\lambda}_3 &= \lambda(A_1 - iA_2) \\
\hat{\lambda}_4 &= -\lambda(A_1 - iA_2) \ .
\end{aligned} \tag{D-11}$$

The general solution is

$$y_{11} = c_1 e^{\hat{\lambda}_1 \psi} + c_2 e^{\hat{\lambda}_2 \psi} + c_3 e^{\hat{\lambda}_3 \psi} + c_4 e^{\hat{\lambda}_4 \psi} \ . \tag{D-12}$$

The substitution of (D-12) in (D-3) leads to

$$\begin{aligned}
d_1 &= \frac{m\bar{P}}{2k} (-1 + iq)\, C_1 \\
d_2 &= \frac{m\bar{P}}{2k} (-1 + iq)\, C_2 \\
d_3 &= \frac{m\bar{P}}{2k} (-1 - iq)\, C_3 \\
d_4 &= \frac{m\bar{P}}{2k} (-1 - iq)\, C_4 \ .
\end{aligned} \tag{D-13}$$

Thus the solution for f_{11} is

$$\begin{aligned}
f_{11} = \frac{m\bar{P}}{2k} \big[& C_1(-1+iq) e^{\hat{\lambda}_1 \psi} + C_2(-1+iq) e^{\hat{\lambda}_2 \psi} \\
& + C_3(-1-iq) e^{\hat{\lambda}_3 \psi} + C_4(-1-iq) e^{\hat{\lambda}_4 \psi} \big] \ .
\end{aligned} \tag{D-14}$$

The real parts of (D-12) and (D-14) are

$$\begin{aligned}
y_{11} = {} & b_1 e^{\lambda A_1 \psi} \cos \lambda A_2 \psi + b_2 e^{\lambda A_1 \psi} \sin \lambda A_2 \psi \\
& + b_3 e^{-\lambda A_1 \psi} \cos \lambda A_2 \psi + b_4 e^{-\lambda A_1 \psi} \sin \lambda A_2 \psi
\end{aligned} \tag{D-15}$$

$$f_{11} = -\frac{m\bar{p}}{2k}\left[(b_1 - qb_2)e^{\lambda A_1\psi}\cos\lambda A_2\psi + (b_2+qb_1)e^{\lambda A_1\psi}\sin\lambda A_2\psi\right.$$
$$\left. +(b_3+qb_4)e^{-\lambda A_1\psi}\cos\lambda A_2\psi + (b_4-qb_3)e^{-\lambda A_1\psi}\sin\lambda A_2\psi\right]. \tag{D-16}$$

A linear function of ψ is added to f_{11} to allow condition (3.2.13) to be satisfied. This gives for the solution

$$\left.\begin{aligned} y_{11} &= b_1 e^{\lambda A_1\psi}\cos\lambda A_2\psi + b_2 e^{\lambda A_1\psi}\sin\lambda A_2\psi \\ f_{11} &= -\frac{m\bar{p}}{2k}\left[(b_1-qb_2)e^{\lambda A_1\psi}\cos\lambda A_2\psi + (b_2+qb_1)e^{\lambda A_1\psi}\sin\lambda A_2\psi\right. \\ &\quad \left. +b_5\psi\right] \qquad (\psi<0) \end{aligned}\right\} \tag{D-17}$$

$$\left.\begin{aligned} y_{11} &= b_3 e^{-\lambda A_1\psi}\cos\lambda A_2\psi + b_4 e^{-\lambda A_1\psi}\sin\lambda A_2\psi \\ f_{11} &= -\frac{m\bar{p}}{2k}\left[(b_3+qb_4)e^{-\lambda A_1\psi}\cos\lambda A_2\psi + (b_4-qb_3)\right. \\ &\quad \left. e^{-\lambda A_1\psi}\sin\lambda A_2\psi + b_6\psi\right]. \qquad (\psi>0) \end{aligned}\right\} \tag{D-18}$$

Case II

$$\frac{4\gamma^2k^2}{m^2\bar{p}^2} < 1 \tag{D-19}$$

Let

$$p^2 \equiv 1 - \frac{4\gamma^2k^2}{m^2\bar{p}^2}. \tag{D-20}$$

Then

$$\hat{\lambda}_{1,2} = \pm\sqrt{\frac{m\bar{P}}{2\gamma^2}}\sqrt{1 \pm p} \,. \tag{D-21}$$

Let

$$A_3 \equiv \sqrt{1 + p} \,, \quad A_4 \equiv \sqrt{1 - p} \,. \tag{D-22}$$

The use of (D-22) allows the roots to be expressed as

$$\left.\begin{aligned} \hat{\lambda}_1 &= \lambda A_3 \\ \hat{\lambda}_2 &= -\lambda A_3 \\ \hat{\lambda}_3 &= \lambda A_4 \\ \hat{\lambda}_4 &= -\lambda A_4 \,. \end{aligned}\right\} \tag{D-23}$$

The general solution for y_{11} is given by (D-12). The solution for f_{11} is found by substituting (D-12) in (D-3) and using the relations for Case II. This leads to

$$\left.\begin{aligned} d_1 &= -\frac{m\bar{P}}{2k} A_4^2 C_1 \\ d_2 &= -\frac{m\bar{P}}{2k} A_4^2 C_2 \\ d_3 &= -\frac{m\bar{P}}{2k} A_3^2 C_3 \\ d_4 &= -\frac{m\bar{P}}{2k} A_3^2 C_4 \end{aligned}\right\} \tag{D-24}$$

therefore the solution for f_{11} is

$$f_{11} = -\frac{m\bar{P}}{2k}\left(A_4^2 C_1 e^{\lambda A_3 \psi} + A_4^2 C_2 e^{-\lambda A_3 \psi} + A_3^2 C_3 e^{\lambda A_4 \psi} + A_3^2 C_4 e^{-\lambda A_4 \psi}\right). \tag{D-25}$$

The renaming of the constants of integration and the addition of a linear function to f_{11} gives

$$y_{11} = b_7 e^{\lambda A_3 \psi} + b_8 e^{\lambda A_4 \psi}$$

$$f_{11} = -\frac{m\bar{P}}{2k}\left(b_7 A_4^2 e^{\lambda A_3 \psi} + b_8 A_3^2 e^{\lambda A_4 \psi} + b_{11}\psi\right) \qquad \text{(D-26)}$$

$$\psi < 0$$

$$y_{11} = b_9 e^{-\lambda A_3 \psi} + b_{10} e^{-\lambda A_4 \psi}$$

$$f_{11} = -\frac{m\bar{P}}{2k}\left(b_9 A_4^2 e^{-\lambda A_3 \psi} + b_{10} A_3^2 e^{-\lambda A_4 \psi} + b_{12}\psi\right) \qquad \text{(D-27)}$$

$$\psi > 0.$$

REFERENCES

1. Lorentz, R., "Achsensymmetrische Verzerrungen in Dünnwandigen Hohlzylindern," Zeit. Ver Deut. Ingr., 52, (1908), 1766.

2. Timoshenko, S., "Einige Stabilitäts Probleme der Elastizitäts-theorie," Zeit. Math. Physik., 58, (1910), 337.

3. Southwell, R. V., "On the General Theory of Elastic Stability," Phil. Trans. Roy. Soc. London, Series A, 213, (1914), 187.

4. Flügge, W., "Die Stabilität der Kreiszylinderschale," Ingenieur-Archiv, 3, (1932), 463-506.

5. Timoshenko, S., and Gere, J. M., The Theory of Elastic Stability, McGraw Hill, Inc., 1961.

6. Fung, Y. C., and Sechler, E. E., "Instability of Thin Elastic Shells," Proceedings of the First Symposium on Naval Structural Mechanics, Stanford University, (August, 1958), 115-168.

7. Lundquist, E. E., "Strength Tests of Thin Walled Duraluminum Cylinders in Compression," NACA Rep. 473, 1933.

8. Donnel, L. H., "A New Theory for the Buckling of Thin Cylinders Under Axial Compression and Bending," Trans. of ASME, 56, (1934), 795.

9. von Kármán, T., and Tsien, H. S., "The Buckling of Thin Cylinderical Shells Under Axial Compression," J. Aero. Sci., 8, No. 8, (1941), 302.

10. Leggett, D. M. A., and Jones, R. P. N., "The Behavior of a Cylindrical Shell Under Compression When the Buckling Load has been Exceeded," Rand M 2190, British Aero, Res. Comm., 1942.

11. Michielson, H. F., "The Behavior of Thin Cylindrical Shells After Buckling Under Axial Compression," J. Aero. Sci., 15, No. 12, (1948), 738.

12. Kempner, J., "Postbuckling Behavior of Axially Compressed Circular Cylindrical Shells," J. Aero Sci., 21, No. 5, (1954), 239.

13. Almroth, B. O., "Postbuckling Behavior of Axially Compressed Circular Cylinders," AIAA, 1, No. 3, (1963), 630.

14. Donnell, L. H., and Wan, C. C., "Effect of Imperfections on Buckling of Thin Cylinders and Columns Under Axial Compression," J. Appl. Mech., 17, No. 1, (1950), 73.

15. Koiter, W. T., "Elastic Stability and Postbuckling Behavior," presented at First All-Union Congress of Theoretical and Applied Mechanics, Moscow, 1960.

16. Kadashevich, Iu. I., and Pertsov, A. K., "On the Loss of Stability of Cylindrical Shells Under Dynamic Loading," IZV. AKAD. SSSR. Oclt. Tekhn. Nauk. Mech., Mashinosti, No. 3, (1960), 30-33, Translation in American Rocket Society Journal Supplement, 32, No. 1, (January, 1962), 140-143.

17. Agamirov, V. L., and Volmir, A. S., "Behavior of Cylindrical Shells Under Dynamic Loading by Hydrostatic Pressure or by Axial Compression," Translation in American Rocket Society Journal Supplement, January, 1961.

18. Yao, J. C., "The Dynamics of the Elastic Buckling of Cylindrical Shells," Proc. of the Fourth U. S. Nat. Cong. of Appl. Mech., 1, (1962), 427.

19. Friedrichs, J. C., "On the Minimum Buckling Load for Spherical Shells," Th. von Kármán Anniversary Volume, Cal. Inst. Tech., Pasadena, (1941), 258-272.

20. Friedrichs, K. O., and Stoker, J. J., "The Non-Linear Boundary Value Problem of the Buckled Plate," Proc. of the Nat. Acad. of Science, 25, (1939), 535.

21. Friedrichs, K. O., and Stoker, J. J., "Buckling of a Circular Plate Beyond the Critical Thrust," J. of Appl. Mech., 9, (1942).

22. Fung, Y. C., and Wittrick, W. H., "A Boundary Layer Phenomenon in the Large Deflection of Thin Plates," Quart. J. of Mech. and Appl. Math., 8, (1955), 338.

23. Masur, E. F., and Chang, C. H., "Development of Boundary Layers in Buckled Plates," J. of the Engineering Mechanics Division, ASCE, 90, No. 2 (1964), 33.

24. Reiss, E. L., "A Theory for the Small Rotationally Symmetric Deformations of Cylindrical Shells," Comm. on Pure and Appl. Math., 13, (1960).

25. Reiss, E. L., "On the Theory of Cylindrical Shells," Quart. J. of Mech. and Appl. Math., 15, (1962).

26. Johnson., M. W., "Boundary Layer Theory for Unsymmetric Deformations of Circular Cylindrical Elastic Shells," J. of Math. and Physics, 42, No. 3 (1963), 167.

27. Donnell, L. H., "Stability of Thin Walled Tubes Under Torsion," NACA Rep., 479, 1933.

28. Marguerre, K., "Zur Theorie der Gekrümmten Platte Grosser Formänderung," Proc. of 5th Inter. Cong. of Appl. Mech., (1938).

29. Yoshimura, Y., "On the Mechanism of Buckling of a Circular Cylindrical Shell Under Axial Compression." NACA TM 1390, 1955.

30. Coppa, A. P., "The Buckling of Circular Cylindrical Shells Subject to Axial Impact," NACA TN D1510, Collected Papers on Shell Structures, (1962), 361.

31. Tennyson, R. C., "A Note on the Classical Buckling Load of Circular Cylindrical Shells Under Axial Compression," AIAA, 1, No. 2, (1963), 475.

32. Carrier, G. F., "Boundary Layer Problems in Applied Mechanics," Advances in Applied Mechanics, III, Academic Press Inc., (1953), 1-18.

33. Sanders, J. L., "Nonlinear Theories for Thin Shells," Quarterly of Applied Math., 21, 1, (1963), 21-35.